Exploration Geophysics (1992) 23, 589–617

The Geophysical Responses of Buried Drums — Field Tests in Weathered Hawkesbury Sandstone, Sydney Basin, NSW

D. W. Emerson, J. E. Reid, D. A. Clark*, M. S. C. Hallett, P. B. Manning

Department of Geology and Geophysics
University of Sydney
NSW 2006

**CSIRO Division of Exploration Geoscience*
PO Box 136
North Ryde, NSW 2113

Abstract

Field and laboratory experiments and tests were carried out to investigate the response of buried steel and plastic drums to the magnetic, transient electromagnetic and resistivity profiling techniques in a magnetically quiet weathered Hawkesbury Sandstone environment in the central Sydney Basin. Steel drums, 200 l, 50 l, 20 l, and 5 l in size, and plastic containers, 70 l, and 20 l in size, were used as buried targets in controlled profiling surveys. The proton precession magnetic method located individual drums buried at shallow depths but with increasing difficulty as drum size decreased. The survey profiles provided data that could be modelled by sphere or dipole sources magnetized by induction as viscous and permanent magnetization contributions were minor. Clusters of buried drums were readily detected by magnetometry and the data successfully modelled with an array of dipole sources. The TEM method clearly located individual steel drums, but the drum anomaly was less evident in the Wenner resistivity data. Plastic drums were not detected by any of the methods applied. Magnetic surveying is the primary method of choice for the location of shallowly buried steel drums in environmental studies.

Key words: drum search, steel drum, plastic drum, magnetic survey, proton precession magnetometry, TEM surveying, resistivity profiling, drum magnetization, steel magnetization, drum anomaly, drum modelling, magnetic modelling, Hawkesbury Sandstone, environmental geophysics

Introduction

Environment studies are readily addressed by geophysical methods which are employed as non-invasive and cost effective techniques in preliminary assessments of contaminated or possibly contaminated lands (Parker, 1992). A common problem is the location of buried containers in surveys of waste, industrial and clandestine disposal sites (Schlinger, 1990). Metallic and plastic drums give frequent cause for concern as they can contain hazardous fluids that may leak into sensitive environments. Magnetic and electromagnetic methods are often applied in the search for buried drums, but little specific information has been published on their field-geophysical responses.

Breiner (1973) noted that a compact buried iron or steel object may be modelled as a dipole source which generates a maximum magnetic anomaly, at a surface observation point, that may be computed approximately by dividing the object's magnetic moment (in appropriate units) by the cube of the distance from the centre of the source to the magnetic sensor. The magnetization of the ferrous material multiplied by its volume (or its mass, in grams, divided by its density, around 8 g/cm^3) gives the moment, which typically ranges between 10^5 and 10^6 Gcm^3 [100-1000 Am^2, SI] per tonne. One tonne of iron can generate an anomaly of about 100 nT (1 nT = 10^{-5} G = 1 gamma, CGS) at 8 metres; this diminishes to about 1 nT (gamma) at 40 metres. Variations to these illustrated values may be encountered. A multiplicity or array of buried iron and steel objects will cause an approximately additive response at the sensor. Quite complex magnetic patterns can be generated depending on the mass, geometry, depth and magnetization of each ferrous source, and interactions between them.

Permanent magnetization (remanence) and demagnetization effects in drum materials need to be considered (Breiner, 1973). Often, an effective susceptibility may be employed to incorporate static and dynamic magnetizations. A hard steel may have a relatively low intrinsic susceptibility of ~1 G/Oe [13 SI], but have a strong remanent magnetization that exceeds the induced magnetization by a factor of up to ~50; soft iron or mild steel typically has an intrinsic susceptibility of ~10 G/Oe [~130 SI] and a relatively low remanent intensity. Demagnetization will act through the susceptibility to reduce the induced and remanent magnetizations and lower the magnitude of the expected anomaly. The observed susceptibility is the intrinsic susceptibility, k_i, divided by [1 + Nk_i], where N is the demagnetizing factor. It follows that the maximum effective susceptibility is 1/N, for very high intrinsic susceptibilities. For spherical sources N = $4\pi/3$ Oe/G = 1/3 SI. Some steels have low magnetizations; rusted, corroded steels, manganese steels and stainless steels may be weakly or very weakly magnetic. Aluminium metal is virtually non magnetic, as are the commonly used polyvinyl chloride and polythene thermoplastics.

Tyagi *et. al* (1983) and Lord and Koerner (1990) presented the results of geophysical search methods applied to drum location in four environments. Magnetic, electromagnetic induction, metal detection and ground penetrating radar methods were used to look for buried drums in quarry sand, ocean bay island sand, noisy (metallic-contaminated) clay and water sites. In clean sites the magnetic techniques detected drums at shallow depths. A 30 nT anomaly was recorded for a 30 (US) gallon (113.6 l) steel drum buried in sand at a depth of 6 ft (1.8 m), but 5 (US) gallon (18.9 l) steel drums under 3 ft (0.9 m) of water cover were not detected. The proton precession magnetometer sensor heights were not clearly specified. Frequency domain electromagnetics detected a 55

(US) gallon (208.2 l) steel drum under 4.5 ft (1.4 m) of sandy cover as did the metal detector, but galvanic resistivity, using a 2.4 m Wenner electrode spacing, failed to detect the drum. Shallowly buried plastic drums, irrespective of their fluid contents, could not be located by magnetics, electromagnetics or metal detection. In the more resistive environments ground penetrating radar located steel and plastic drums buried at shallow depths; plastic drums containing salt water gave better responses than those filled with fresh water or air.

Gilkeson *et. al* (1992) carried out field test studies on a 55 (US) gallon (208 l) steel drum with proton precession magnetic and frequency domain electromagnetic (terrain conductivity meter) instruments. They measured a maximum anomaly of 57 nT under an elevated drum, the bottom of which was 3.1 m above the sensor. Their work indicated that, for clean sites, magnetics might detect a buried drum to about 4.5 m below the sensor and electromagnetics might sense it down to about 2.5 m if the surroundings were resistive. They used the magnetic field test results to calibrate a theoretical magnetic model which suggested that a 3 m field grid would generally be adequate for drum location detection; for definition, a 1.5 m grid would be optimum. In magnetization tests on two rotated drums, they did not observe permanent magnetization in either a drum with a welded top or in a drum with a removable top secured by a steel collar. However, the drum with the removable top did exhibit hysteresis in that a negative anomaly was measured when the drum was first rotated and four hours later a positive anomaly was observed. It was proposed that the transition from negative to positive values reflected an adjustment of magnetic domain walls within the steel, in response to the earth's magnetic field.

For very large "drums", Schlinger (1990) indicated that magnetic anomalies of the order of 3000 to 5000 nT could be expected from underground steel storage tanks with capacities in 4000 to 40,000 l range, when such tanks were buried about 1 m below the ground surface.

Currently there appear to be four generally accepted or established geophysical methods used in drum search. These are: the magnetic technique (MAG), using total field or vertical gradient anomalies measured by proton precession magnetometers; the frequency domain electromagnetic induction technique (EMI), using terrain conductivity meters operating at about 10 kHz; suitable metal detectors (MD); and ground penetrating radar (GPR) operating at about 100 MHz. Ideally, all four techniques should be employed in site studies. The EMI and GPR techniques certainly provide useful information in many sites but the GPR and some EMI devices can be relatively expensive and they do not work well in conductive environments. The MD method is rapid, but qualitative and depth-limited. Anecdotal evidence suggests that some MD instruments may detect 200 l metal drums buried at about 1 m depth. For ease of deployment, speed of data acquisition, convenience of qualitative data interpretation and low capital and operating costs the MAG method has advantages in the search for buried ferrous drums especially in reconnaissance work.

The aim in drum-site magnetic surveys is to locate a steel drum or cluster of steel drums and to try to estimate the depth(s) of burial. Depth estimation may be difficult in the absence of auxiliary information, even on a clean site, owing to the potential field ambiguity problem; on noisy sites it may be impossible owing to the composite and complex nature of the anomalies. However, for well defined anomalies a maximum depth to source can be estimated, which may be useful information in this context. In considering the magnetic response of drum the site location needs to be specified so that the earth's inducing magnetic field characteristics may be ascertained The magnetic nature of the burial medium controls subsurface magnetization contrasts. The magnetic response also depends on the drum's geometry, dimensions, mass, fabrication material, orientation, depths below ground surface and magnetic sensor and co-ordinates of the drum with respect to survey traverse lines. There is little basic information on magnetic characteristics available in the literature. In EMI and GPR surveys the electric and dielectric properties of the burial medium may be important, as too can the contents of the drum.

This paper describes the results of the field magnetic experiments on a variety of commonly used drums. The proton precession magnetometer field work recorded, and the interpretations dealt with, total magnetic intensity anomalies. Magnetic field gradients were not studied. Some transient electromagnetic (TEM) and galvanic resistivity measurements were also made. The purpose of the study was to augment the sparse drum-search data and contribute to improved interpretations of drum-site data.

Drum Site Survey Details

The Sydney Basin test site was located in weathered Triassic Hawkesbury Sandstone on a ridge 100 m above the east bank of the Hawkesbury River, 53 km northwest of Sydney, New South Wales. The approximate magnitude of the earth's magnetic field at the site is 58,000 nT (gammas, CGS) with an inclination of −64.5° and a declination of 12°E.

Magnetic and mass physical property laboratory measurements were carried out on samples of excavated soil and weathered rock; these are summarised in Table 1. Magnetic susceptibility readings were taken with a hand-held bridge at many surface locations. Susceptibilities were quite low usually except where a thin (1 cm) broken-up layer of laterized sandstone was encountered. As can be seen from the reported values in Table 1, this veneer can carry substantial induced and remanent magnetizations and contributed to the background geological noise in the study. However, the occurrence of this material on the test site tended to be erratic and its effect minor. The laterite was probably developed during the Miocene (D. F. Branagan, pers. comm.) when substantial horizons were formed on the Sydney Basin landforms.

Four electrode galvanic resistivity tests conducted at 1 kHz in the laboratory showed that samples of soil and weathered rock had moderate resistivities (Table 2). The soil and weathered rock comprised mainly fine quartz grains with minor ferruginous and clay materials.

Five site areas were selected for drum location in a 4 hectare tract. The details of the sites and drums are given in Table 3. A pocket magnet adhered strongly to all the steel drums

TABLE 1
Magnetic properties and mass properties of some site materials.

Material (weathered samples)	Magnetic susceptibility		Natural remanent magnetization	Density bulk	Porosity apparent
	CGS × 10^{-6} (μG/Oe)	SI × 10^{-6}	μ gauss (CGS) mA/m (SI)	g/cm^3 (t/m^3)	%
Area A					
Hawkesbury Ss no. 1	3	38	8	2.22	17.8
Hawkesbury Ss no. 2	6	75	4	2.14	21.0
Area C					
Laterized Ss no. 1	1285	16,148	1624	2.81	7.7
Laterized Ss no. 2	58	729	147	2.57	12.7
Area B					
Sandy soil no. 1	5	63	60	1.52	n.a.
Sandy soil no. 2	5	63	1	1.56	n.a.

TABLE 2
Laboratory determined soil/sand profile resistivities.

Approximate Depth (cm)	Sample Description	Resistivity (Ωm)
Area B 15	humic soil (slightly moist)	540
Area B 30	quartz sand with ferrous clay coating (moist)	154
Area B 60	as above	223
Area B 85	as above	178
Area E 10	humic soil (quite moist)	140
Area B 0	weathered sandstone bedrock	314

TABLE 3
Site details — survey areas and drum specifications.

Area	Field Tests	Drum, Nominal Capacity	Drum Mass (empty) kg	Drum Dimensions (external) H: height, D: diameter; cms	Depth of Burial to Top of Drum	Comments
A	Magnetic	200 l, steel	18.0	H:88, D:58	0.00m (in cleft in weathered sandstone platform)	common heavy duty industrial "44 gallon" petrol drum, exterior painted
B	Magnetic, resistivity, TEM	50 l, steel	3.8 incl. lid	H:48, D:37	0.35 m (in sandy soil)	calcium hypochlorite "chlorine" drum with detachable lid, exterior and interior painted
	Magnetic	200 l, steel	14.5 to 21.0	Similar to A	0.2 m	multiple drum tests
C	Magnetic	20 l, steel	1.7	H:35, D:29	0.30 m	partly painted, slightly rusted kerosene tin
		5 l, steel	0.5	H:27, D:15.5	0.35 m (in sandy soil)	partly painted, motor mower fuel mixing can
D (noisy)	Magnetic	20 l, steel (not same drum as in area C)	1.8	H:35, D:29	0.30 m	partly painted, slightly rusted kerosene tin
		5 l, steel	0.5	H:22.5, D:17	0.30 m (in sandy soil)	partly painted, slightly rusted mixing can
E	TEM	20 l, plastic	1.4	H:35, base 26×2	0.30 m	black polythene, acetic acid container,
		70 l, plastic	2.5	H:60, D: ~32	receiver placed 0.30 m above	"dangerous goods" grade blue utility container, lightweight
		20 l, steel	1.75	H:35, D:29	0.30 m	kerosene tin
		5 l, steel	0.5	H:27, D:15.5	0.30 m (in sandy soil)	mixing can

which also showed excellent electrical continuity when ohmmeter probes scratched through surface paint and rust. In all areas the attitude of the drums was vertical; in area A the drum was also tested in a horizontal position. Areas A, C, D and E were surveyed with single-profiles; area B was surveyed with multiple profiles. Each area was magnetically surveyed before and after drum placement.

Total magnetic intensity measurements were made, on stations at 1 m or less separation on the traverse lines, with a Geometrics G-856 proton precession magnetometer readable to 0.1 nT. The staff-mounted magnetic sensor was held at 1.5 m, 2.5 m and 3.5 m elevations along the traverses. Diurnal variations were monitored by frequent returns to a central base station. Diurnal changes were minor. After the layout of the survey lines, readings could be taken about every half minute for the 1.5 m and 2.5 m sensor staff heights and about every minute for the 3.5 m staff for 1 or 2 m station spacings.

TEM measurements on Areas B and E in this study were carried out using a Geonics EM-47 transmitter and PROTEM receiver. The EM-47 transmitter has an extremely rapid turn-off time, thus enabling very shallow depth sounding and profiling to be carried out. For the 5 m × 5 m transmitter loop employed in this survey, the turn-off time was 0.42 μsec. Transmitter current was set at 2.0A. The receiver was the standard Geonics PROTEM high frequency coil, with an effective area of 31.4 m^2. Profiles were recorded over four different buried drums, and the transient ground response recorded at 19 gates at each receiver station. The absolute value of the voltage responses are plotted in the TEM profiles presented in this paper, i.e. positive and negative values are not identified except for the transient decay examples presented in Figure 20 b. The gate centre times (refer Appendix) ranged from 6.9 μsec at channel 1 to 561 μsec at channel 19. A Slingram transmitter-receiver configuration, shown in Figure 20a, was used for all TEM measurements in this study, with the transmitter and receiver centres separated by 12.5 m. The small size of the transmitter loop meant that profiling could be carried out relatively rapidly by two operators. The average time required to make two readings and to move the transmitter and receiver to the next station was 6 minutes.

Galvanic resistivity measurements were made along the central traverse of Area B. An ABEM Terrameter was used with Wenner electrode configurations with spacings of 1, 2 and 3 m.

Figures 1 to 4 present views of the drum burial at site B and the field operation of the proton precession magnetometer at site B and the PROTEM receiver at site E. Table 4 summarises details of the traverse lines on the five drum areas.

Field Results-Magnetics; Areas, A,B,C,D

Drum anomaly characteristics for Areas, A, B, C, D are given in Table 5 which cites the maximum total magnetic intensity anomaly and half-width for each test. The exact half-widths of the drum anomalies were difficult to determine owing to minor background effects. In an applied geophysics sense, the individual drum anomalies are not large in magnitude, increasing with drum size from a few nT to 130 nT. In plan, the anomalies are quite small in area as the half-widths show (the half-width is half the anomaly width at the half maximum amplitude). The anomaly positive peaks are flanked by associated minor negative troughs to the south. These negatives are readily seen in the cases of the 200 l drum in Area A and the multiple 200 l drums in Area B; they are barely discernible for the smaller drums owing to the effects of background noise.

Area A, 200 l steel drum

The Area A 200 l drum anomalies are shown in Fig. 5. The anomalies are prominent and range from 33 to 100 nT in amplitude depending on drum orientation and sensor clearance. In the horizontal attitude the drum's long axis was parallel to the ground and normal to the traverse direction. The horizontal orientation anomalies are about 20 per cent less than those measured for the vertical orientation of the drum. Tyagi *et. al* (1983) noted a dependence of the magnetic anomaly on drum orientation.

TABLE 4
Traverse line details.

Area	Traverse Bearing	Comments
A	331°mag., NNW-SSE	single traverse on Hawkesbury Sandstone over 200 l steel drum in cleft
B	047°mag., NE-SW	ten traverses, each separated by 1 m, on sandy soil over 50 l steel drum
B	050°mag., NE-SW 000°mag., N-S	elevated traverses on wood planks between aluminium ladders over single 200 l steel drums and a 3 × 3 cluster of 200 l steel drums (~20 cm clearance between plank top and drum tops), these traverses were located away from the 50 l drum site
C	315°mag., NW-SE	single traverse on sandy soil over 20 l and 5 l steel drums
D	312°mag., NW-SE 000° mag., N-S	two traverses on sandy soil over sandstone (probably containing a lateritic or ironstone band) over 20 l and 5 l steel drums
E	048°mag., NE-SW	single traverse on moist sandy soil over a 20 l plastic drum and over a 70 l plastic drum and over 20 l and 5 l steel drums
Earth's inducing magnetic field at the site: 58,000 nT magnitude 12°E declination -64.5° inclination		

FIGURE 1
Buried 50 l chlorine drum at site B with one metre yardstick over top of hole which was subsequently filled in prior to geophysical tests.

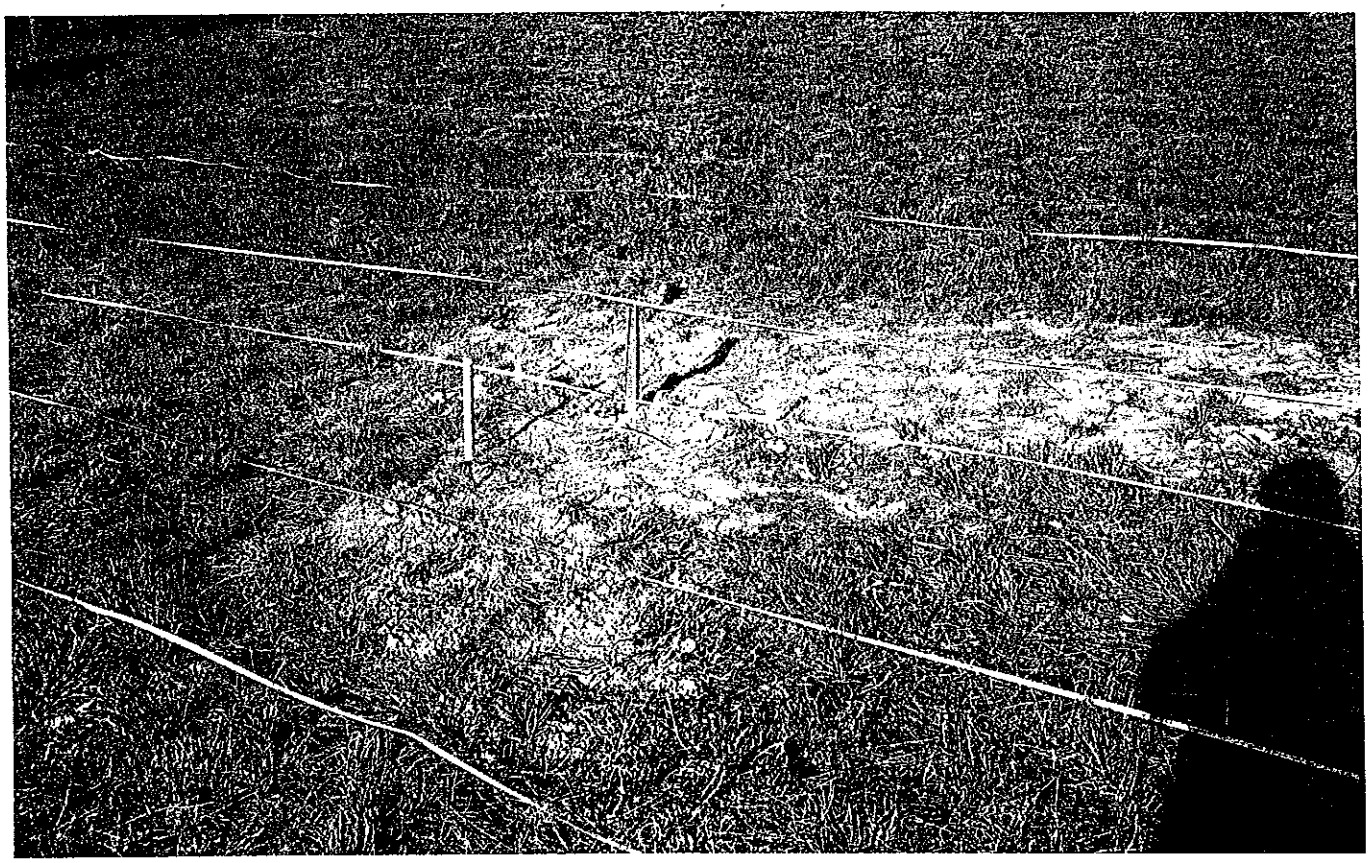

FIGURE 2
Taped survey lines, one metre apart, running 047° magnetic azimuth (to the left hand side) over the site B buried 50 l drum marked by the large peg. The smaller peg to the north located the maximum magnetic anomaly recorded at 2.5 m sensor height.

FIGURE 3
P. Manning holds the staff and M. Hallett notes the field readings for the site B magnetic surveying with 2.5 m sensor height.

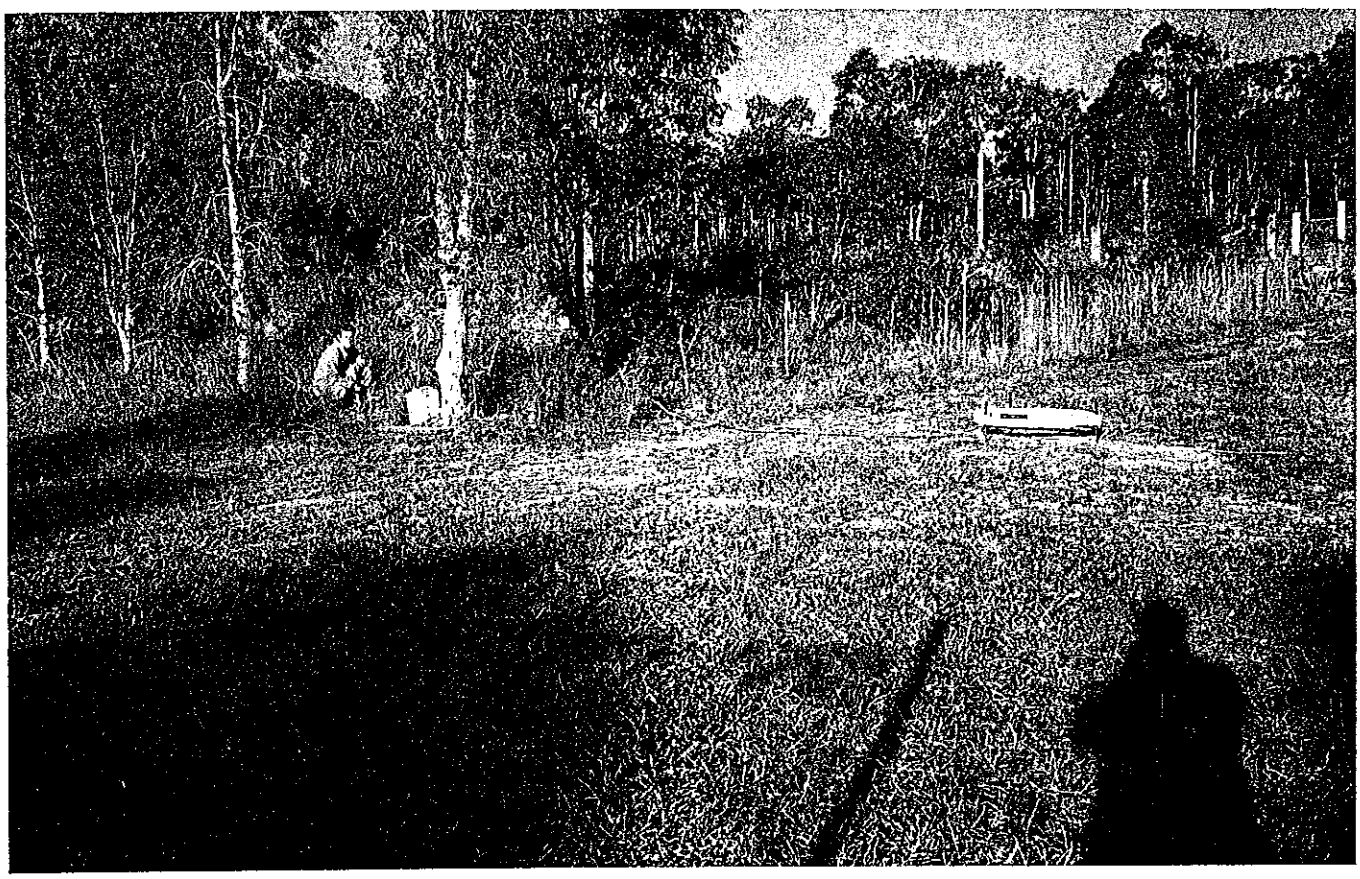

FIGURE 4
J. Reid records readings from the PROTEM receiver at site E. The receiver coil is over a buried plastic drum.

TABLE 5
Summary of total magnetic intensity anomaly responses from buried drums.

Area	Drum (steel)	Sensor height above drum top level, m	Maximum anomaly nT (gamma, cgs)	Anomaly half-width m (approx.)	Comments
A	200 l vert.	2.50	100	1.7	anomaly maxima shifted
	200 l vert.	3.50	44	2.0	0.5 m (magnetic)
	200 l hor.	2.50	82	1.7	northerly from drum
	200 l hor.	3.50	33	2.0	centre, slight variations in maxima when drum rotated (see text)
B	50 l vert.	1.86	62	1.2	refer to Figs 6 and 7
	50 l vert.	2.86	22	1.6	
	50 l vert.	3.86	11	2.0	
C	20 l vert.	1.80	15	1.1	very erratic background
	20 l vert.	2.80	8	1.4	noise (±10 nT)
	20 l vert.	3.80	~3		(ironstone rubble) rendered difficult the
	5 l vert.	1.85	15	0.7	definition of smaller
	5 l vert.	2.85	~5		anomalies along the
	5 l vert.	3.85	~2		profile, anomaly maxima shifted 0.5 m (magnetic) northerly from drum centres
D	20 l vert.	1.80	32	1.0	area D straddles a sharp
	20 l vert.	2.80	12	1.5	30 nT anomaly interpreted as due to
	5 l vert.	1.80	13	1.0	shallow ironstone band
	5 l vert.	2.80	6		in/on underlying sandstone, drum burial was on the steep anomaly flank
B	200 l vert.	2.67 to 2.76	range: ~0 to 133	~1.6	nine (9) individual drums
	200 l vert.	2.7 3.7	525 (N-S) 212 (NE-SW)	1.8 2.5	the nine (9) drums in a 3 × 3 cluster

The drum had a welded top with plug and bung holes. It had been stored for several years in an upright position near the test site. The nominal magnetic profile over the vertical drum, shown in Fig. 5, was measured with the drum upright and a line from the drum centre to the plug hole pointing approximately towards magnetic north. In measurement experiments lasting two hours, the drum was rotated about its long axis and also about its diameter. For the 2.5 m sensor clearance, a maximum anomaly of 100 nT was measured with plug hole pointing to magnetic north, and a maximum of 106 nT observed with the plug pointing eastwards. On inverting the drum the maximum anomaly diminished to 86 nT with the plug pointing eastwards and to only 71 nT with the plug pointing northwards.

For the horizontal drum, the nominal magnetic profile, shown in Fig. 5, was for the welded top pointing westwards and the plug hole uppermost — the maximum anomaly for this setup was 82 nT. Only minor anomaly variations were noted when the drum was rotated about its long axis.

It would appear that induction is the major component of the 200 l drum's total magnetization. It might be expected that domain well readjustment would eventually align the remanent magnetization with the earth's field direction (Gilkeson *et. al*, 1992).

It is clear that 200 l steel drums are readily detectable with 2.5 m and 3.5 m magnetic sensor elevations in the burial situation described in this study.

Area B, 50 l steel drum

Most of the magnetic survey effort was expended on Area B where the drum was buried at 29.85 m traverse (×) distance on line 0 and covered with 0.35 m of sandy soil. Ten northeast-southwest traverses, one metre apart, were surveyed with 1.5, 2.5 and 3.5 m sensor terrain clearance and station spacings of 0.5 or 1.0 or 2.0 m depending on location. Background noise was identified, at 2.5 m sensor terrain clearance, within a 10 nT band, prior to drum emplacement. The results of the survey are shown in Fig. 6 as profiles and in Fig. 7 as contours of relative total magnetic intensity.

Profiles and contours for the 1.5 and 2.5 m sensor elevations clearly show small, compact but recognisable magnetic anomalies, with recorded magnitudes of 62 and 22 nT. The 3.5 m sensor elevation data show a barely discernible 11 nT

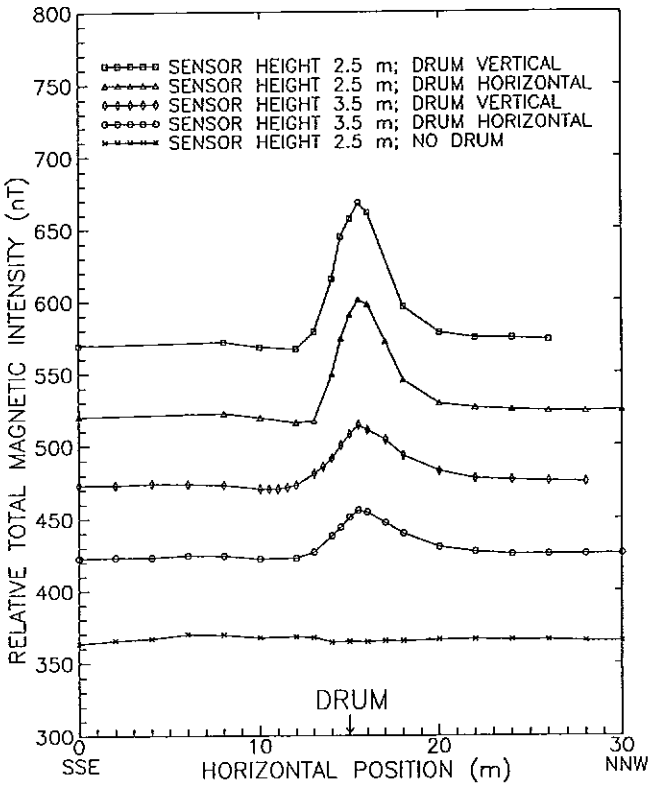

FIGURE 5
Total magnetic intensity anomaly profiles from site A where a 200 litre (44 gallon) steel drum was located in a rock cleft. The profiles have been arbitrarily separated for clarity.

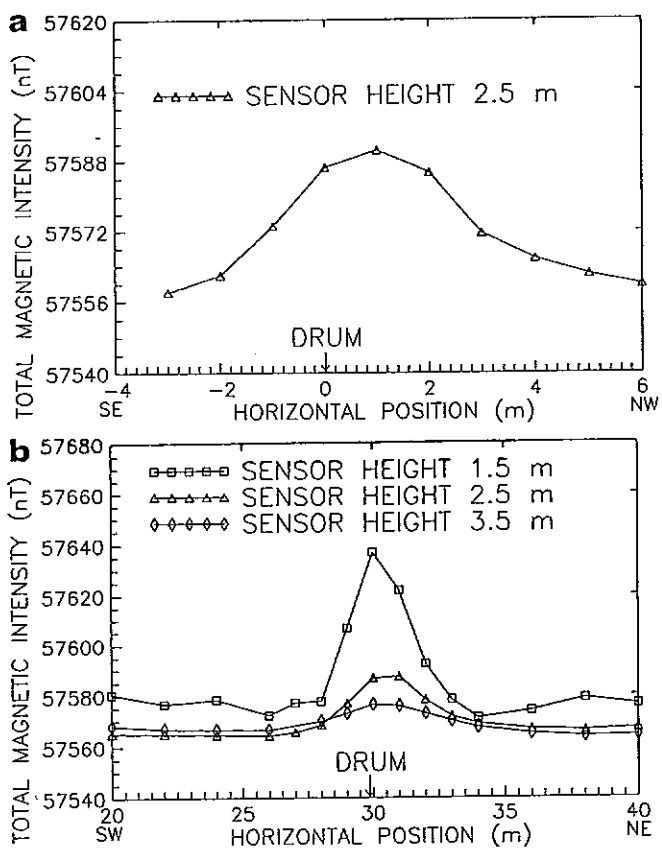

FIGURE 6
Total magnetic intensity anomaly profiles from site B over a buried 50 l steel drum with its top 35 cm below the surface. The top profile (a) runs northwest-southeast; the bottom profiles (b) run northeast-southwest and show the effects of sensor height.

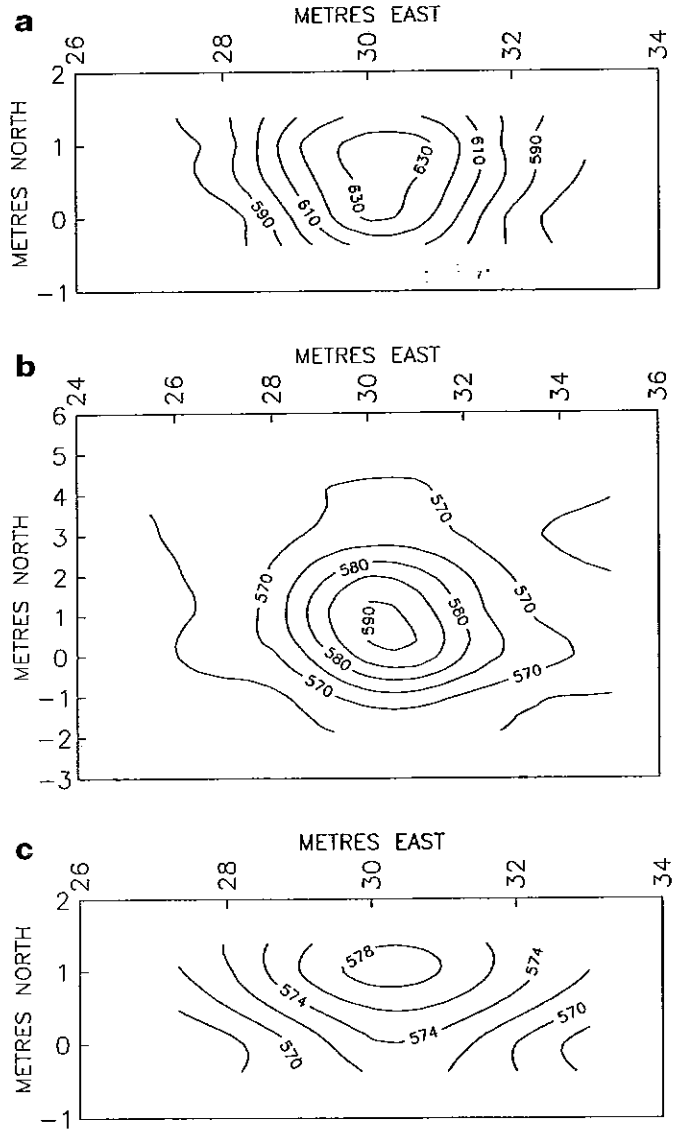

FIGURE 7
Contours of anomalous total magnetic intensity over the 50 l steel drum buried at 35 cm depth (to top) in site B. The base levels are arbitrary. The top (a), middle (b) and bottom (c) profiles show the effects of increasing the sensor height.

anomaly. These anomalies were recorded along traverse 0 and they are not necessarily the absolute maximum anomalies. For the 2.5 m sensor elevation, the absolute maximum anomaly of 28 nT was located 0.7 m from the drum centre on a bearing of 330° magnetic, 30° away from magnetic north. Nevertheless, the overall appearance of the anomalies suggests that induction is dominant. The data presented in Figs 6 and 7 relate to the stations established on the regular survey lines — no attempt was made to define the anomaly in great detail. However, it was noted that for the 50 l drum, minor irregularities in the station location and bending or non-verticality of the sensor staff will lend to minor variations in the recorded anomalies. It is not routinely feasible to endeavour to define perfectly this type of anomaly with a minuscule grid, rather the anomaly location and reasonable delineation should be the aim in drum search.

The survey results show that 50 l drums are fairly readily detectable with 1.5 m and 2.5 m magnetic sensor elevations for the burial situation described in this study.

Areas C and D, 20 l and 5 l steel drums

The profile data for the small drums are presented in Fig. 8. The 20 l and 5 l drum surveys were troubled by geological noise on both Areas C and D. In Area C the excavation of the emplacement hole disturbed a near surface ironstone rubble layer and thus the hole itself generated a minor anomaly while it was open. This, coupled with natural anomaly variations along the traverse and the relatively low magnetic effects of the drums, made the confident definition of the anomalies difficult to attain even with the experimental controls available. In Area D the situation was worse because the site was located on a linear magnetic feature, presumably an ironstone band in the sandstone bedrock. The results from these two areas represent the limits of small drum detectability in an environment of low to moderate natural magnetic noise. Repeatability of measurements was of the order of ±3 nT at 1.5 m sensor height.

For the 20 l and 5 l drums in Area C the anomalies are clear for the 1.5 m sensor elevation, reasonably clear with the 2.5 m sensor elevation and not really discernible with any confidence for the 3.5 m sensor elevation even though small anomalies are apparent (with hindsight). The 20 l and 5 l drums in these tests give very similar anomalies at all sensor elevations, even though the 5 l drum was buried 5 cm deeper and was only 30 per cent of the 20 l drum's mass. The 5 l drum was filled with salty (0.2 ohm m) water in preparation for a TEM test. It is thought the similarity of the magnetic responses is a consequence of a relatively greater magnetization of the 5 l drum steel.

The results from Area D (where different drums were used) in Fig. 8c show slightly greater anomalies for the 20 l drum than were recorded for Area C. When the 20 l drum was inverted the 32 nT anomaly changed to a small negative value in the time frame of the experiment (two hours). The inverted 5 l drum gave an anomaly of 14 nT, about half the magnitude of the 20 l drum at 2.5 m sensor elevation. In the upright position, the 5 l drum produced a small negative anomaly, about −2 nT, in the time frame of the experiment at the 2.5 m sensor elevation.

Although the anomalies in Area D are recognisable with experimental hindsight, it is very doubtful that they would have been identified as drum anomalies in a similar real field situation, i.e. mixed up with a geological anomaly.

Area B 200 l steel drums

Nine 200 l drums were used in an experiment to determine the response of a square 3 × 3 array of vertical drums clustered (on the ground) under a wooden traverse plank supported by aluminium ladders. The drums were then traversed individually. The survey results are presented in Table 6 and Figs 9 and 10 which show prominent anomalies for the drum cluster and an interesting range of anomalies for the individual drums. There is no direct correlation between mass and anomaly size. Owing to field interaction the drum

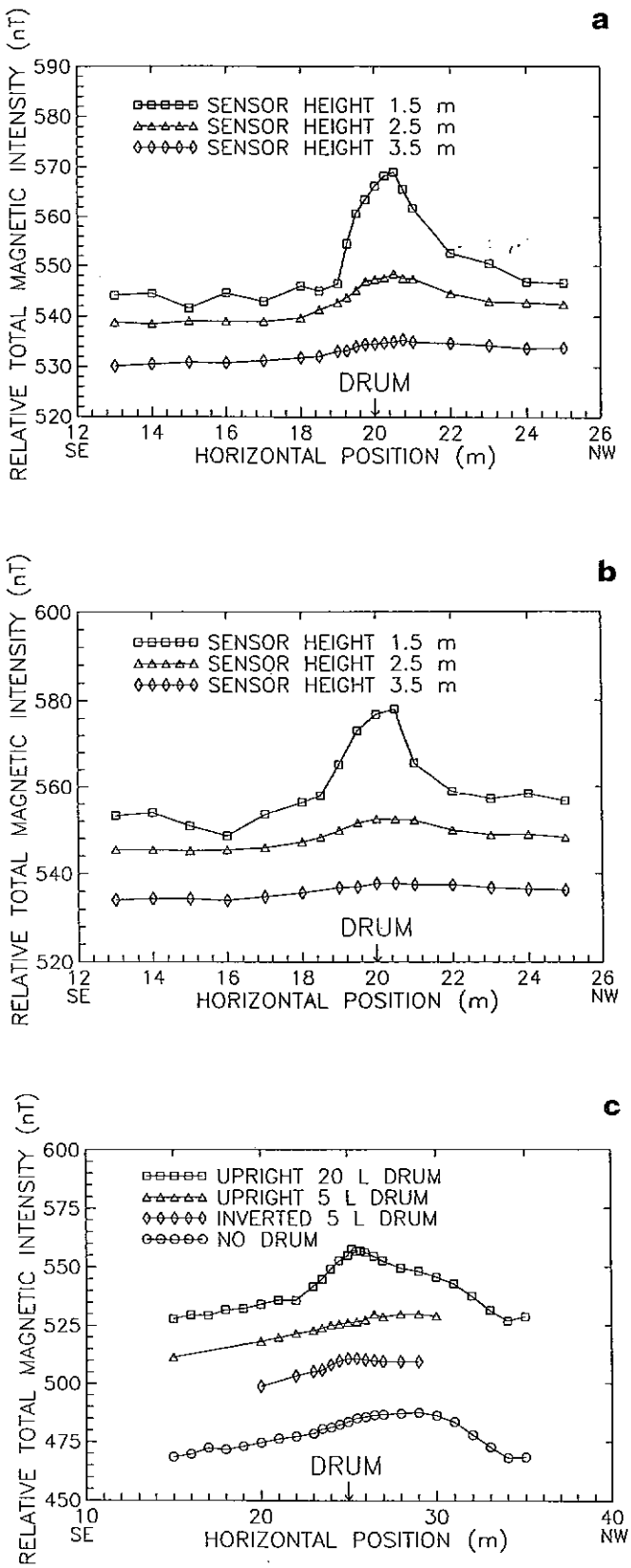

FIGURE 8
Profiles of anomalous total magnetic intensity from sites C and D where 20 l and 5 l steel drums were buried to depths of 30 cm. The recorded base levels have been altered arbitrarily to separate the profiles. The top (a) data sets are for the 20 l site C drum. The middle (b) data sets are for the 5 l site C drum. The bottom (c) data sets are for the relatively noisy site D where readings are shown for 2.5 m sensor height with traverses across buried 5 l and 20 l drums.

TABLE 6
200 l drums — tests at site B.

Drum 200 l	Mass kg	Magnetic anomaly nT at +0.5 m (x)	Comments
1	17.5	89	rusted drum
2	15.5	133	
3	21.0	82	
4	20.0	117	silicone storage drum
5	18.5	0	
6	20.0	116	silicone storage drum
7	17.5	96	
8	14.5	40	slightly rusted
9	18.0	100	used in site A

Notes: i) drums tested with a pocket magnet that adhered strongly to all drums;
ii) all drums lidless except no. 9;
iii) drums 1 to 8 tested inverted with base plates uppermost and stored this way for weeks prior to tests

anomalies are clearly not additive. The maximum recorded anomaly for the 2.7 m sensor height was 525 nT. The individual drums showed a range of anomalies, at the +0.5 m station, from zero to 133 nT, with an average of 86 nT. All drums firmly held a pocket magnet so remanence effects were inferred for the behaviour of drum no. 5 which exhibited no anomaly due to a fortuitous cancellation of the induced magnetization by remanence of approximately equal intensity and opposite direction.

Discussion — Magnetic Field Survey Results

A summary of the total magnetic intensity anomaly profiles is presented in Fig 11. It is evident that the anomaly depends on drum size and burial and sensor height. The magnetic moment of a drum, and consequently the associated anomaly, is proportional to its mass. The anomaly magnitude varies approximately as the inverse cube of the distance of the sensor from the drum. These factors generally result in the ready detectability of 200 l and 50 l steel drums within a few metres of the sensor. However, as Table 6 shows, considerable magnetization variations seem to be able to occur in a particular class of drum. The smaller 20 l and 5 l steel drums are clearly more difficult to detect even in relatively quiet geological environments. Nevertheless, such drums, if buried at shallow depths, should be detectable by thorough search procedures in quiet areas. A feature common to all the drum profiles is the narrowness of the anomalies — the half-widths are quite limited, 1 to 2 m.

The magnetic results presented herein relate to tests carried out mainly in fairly quiet geological environments without deleterious industrial noise (e.g. powerlines) and cultural effects (e.g. steel building frames). The detectability of individual drums in less favourable conditions would be impaired as the results from site D show.

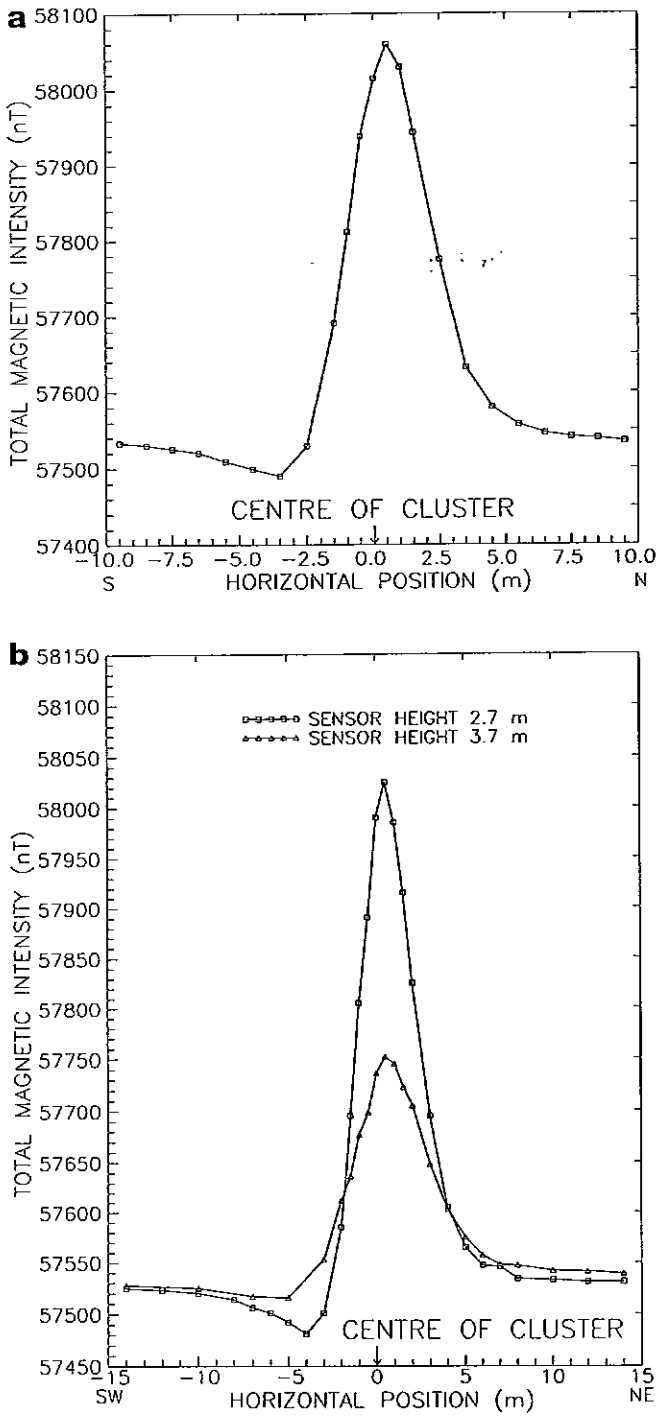

FIGURE 9
Total magnetic intensity anomaly profiles, site B, for a cluster of nine 200 l steel drums in a 3 × 3 array under a wood plank over which magnetic traverses were made in a magnetic north-south direction, shown in the top (a) profile where the sensor height was 2.7 m, and in a northeast-southeast direction for two sensor heights 2.7 and 3.7 m, shown in the bottom (b) profiles.

Clusters of drums, however, can generate quite sizeable anomalies which should stand out against moderate noise if the drums are not too deeply buried. The small half-widths measured at 2.7 and 3.7 m sensor heights indicate that areally compact positive anomalies, with small associated negatives, are likely to be encountered in practice.

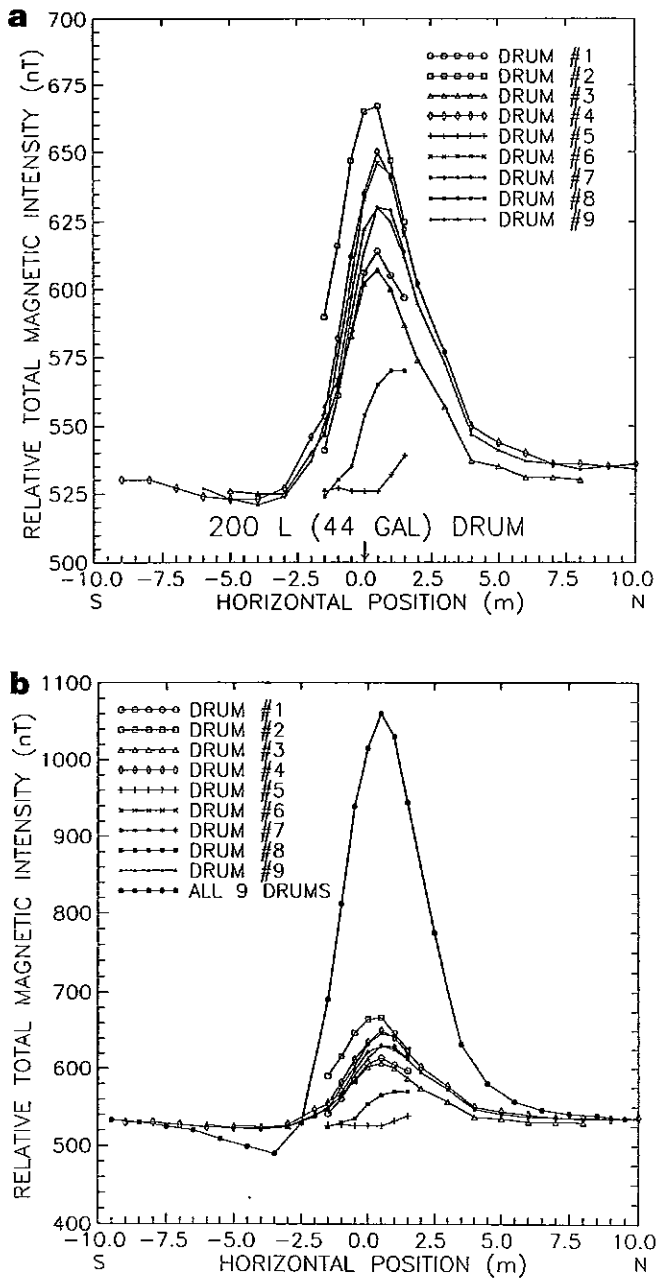

FIGURE 10
Total magnetic intensity north-south anomaly profiles, site B, for each of the nine steel drums used in the cluster measurements. The anomaly of each drum is shown in the top (a) profiles for 2.7 m sensor height. The bottom (b) profiles show the individual and total 3 × 3 array anomalies.

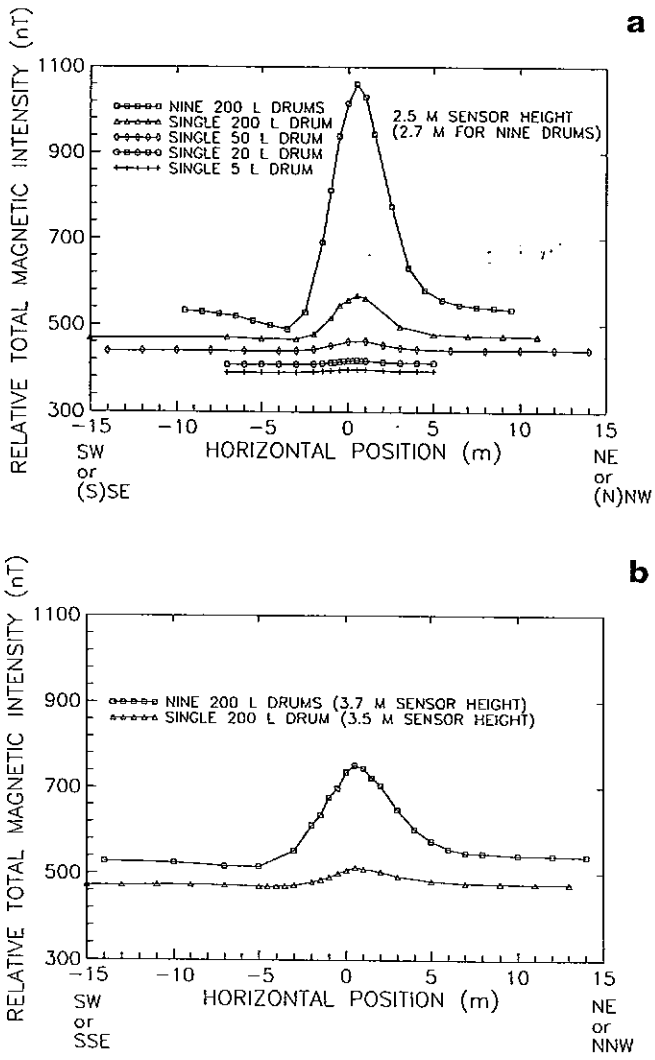

FIGURE 11
Total magnetic intensity anomaly profiles, arbitrarily separated for clarity, showing, at the top (a), the anomalies for 5 l, 20 l, 50 l and 200 l buried steel drums with 2.5 m sensor height and the anomaly for a cluster of 3 × 3 200 l drums with 2.7 m sensor height. A comparison of the anomalies from a single (no. 9) 200 l drum and a cluster of 3 × 3 200 l drums can be seen in the bottom (b) panel.

These comments relate to steel drums buried in a southern hemisphere area with a steep upwards-pointing (negative) magnetic inclination. Care should be taken when using these results to comment on or assess steel drum anomalies from areas with significantly different inducing fields or when applied to drums with dominant permanent magnetizations.

Magnetic Properties of Steel Materials

The magnetic anomaly produced by a buried ferrous source is a function of its depth, size, shape and magnetic properties. The total magnetization is the vector sum on the induced and remanent magnetizations. In the context of drum search, the remanence can be considered to consist of two components:

i) stable remanence or permanent magnetization, which is independent of the ambient field and does not change over the experimental time scale;

ii) viscous remanence, which is only instantaneously independent of the ambient field, but changes measurably over the experimental time scale as the magnetization attempts to re-equilibrate with a changed ambient field, by movement of domain walls (refer to Clark & Emerson, 1991, Fig. 7).

Permanent magnetization is particularly important for hard magnetic materials, including certain steels, which have high coercivity, strong stable remanence and relatively low susceptibility. On the other hand, induced magnetization

dominates for soft magnetic materials, such as soft iron and mild steel. Soft magnetic materials are also more likely to exhibit magnetic viscosity (time-dependent magnetization).

Because induced magnetization and viscous remanence both arise in response to the internal field, they are both directed parallel to this field, provided the magnetic material is isotropic. Thus long-term viscous remanence increases the effective susceptibility of the source and can be incorporated into magnetic models simply by increasing the assumed susceptibility. The effective susceptibility, k_{eff}, is defined by the relationship:

$$J_{IND} + J_{VRM} = k_{eff}F,$$

$$\therefore k_{eff} = (J_{IND} + J_{VRM})/F = k + J_{VRM}/F$$

where k is the ordinary susceptibility, J_{IND} is the induced magnetization, J_{VRM} is the viscous remanence and F is the ambient field.

Assume for simplicity that the ambient field and the magnetization, J, lie along a principal axis of the demagnetizing tensor for the source (e.g. either along the axis or along a radius of a cylindrical drum). The self-demagnetizing field within the source is $-NJ$, where N is the demagnetizing factor along the magnetization direction. The resultant internal field is therefore F-NJ. Viscous remanence continues to build up if, and only if, the resultant internal field is positive, i.e. for $F > NJ$. The maximum (induced + viscous) magnetization occurs when the magnetization has equilibrated with the external field, i.e. when the external field and the self-demagnetizing field cancel to give zero internal field (refer to Figure 12). Therefore

$$J_{IND} + J_{VRM} \leq F/N; \; k_{eff} \leq 1/N.$$

For a spherical body, therefore, where $N = 4\pi/3$ Oe/G (= 1/3 SI), the maximum effective susceptibility, including the effect of viscous remanence, is limited by self-demagnetization to a value of $3/4\pi = 0.239$ G/Oe (= 3 SI). Thus the anomaly due to solid, quasispherical, highly magnetic ferrous objects is greatly reduced by self-demagnetization compared to the anomaly that would be predicted using the intrinsic susceptibility. Anomalies due to rod-like and sheet-like bodies, on the other hand, depend greatly on their orientation with respect to the geomagnetic field. When the long axis of a rod or the plane of a sheet is aligned with the field, very large anomalies are possible, as the demagnetizing factor along these directions is small. For a long rod oriented perpendicular to the field, however, the maximum effective susceptibility is $1/2\pi = 0.16$ G/Oe (= 1/2 SI) and for a thin sheet oriented perpendicular to the field the maximum effective susceptibility is only $1/4\pi = 0.08$ G/Oe (= 1 SI).

The viscous remanence that can be acquired by a compact ferrous source is tightly constrained by self-demagnetization. Consider a spherical source consisting of mild steel with intrinsic susceptibility 8 G/Oe (100 SI). The observed susceptibility is given by $8/[1 + 8(4\pi/3)] = 0.232$ G/Oe [100/(1 + 100/3) = 2.91 SI] and the maximum effective susceptibility (1/N) is 0.239 G/Oe [3 SI]. Thus the contribution of VRM to the effective susceptibility is at most 0.007 G/Oe [0.09 SI], or 3% of the effective susceptibility. Similarly, for a hard steel with low intrinsic susceptibility of 1 G/Oe [12.6 SI], the maximum contribution of VRM to the effective susceptibility is 0.046 G/Oe [0.58 SI]. These results may be expressed alternatively for spherical sources:

$$Q_{VRM} \leq 0.03 \qquad (k_i = 8\text{G/Oe}),$$

$$Q_{VRM} \leq 0.24 \qquad (k_i = 1\ \text{G/Oe}),$$

where Q_{VRM} is the Koenigsberger ratio for VRM, i.e. the ratio of viscous remanence to induced magnetization. Thus VRM makes, at most, only a minor contribution to the total magnetization of a quasispherical ferrous object, although for other geometries, such as hollow drums, with small demagnetizing factors, VRM may be a substantial contributor to the magnetization.

Permanent magnetization (stable remanence) is acquired during cooling of the ferrous material through its Curie temperature, and may be modified during subsequent manufacturing processes, such as rolling, cutting, welding etc. The direction of permanent magnetization reflects the ambient field during its acquisition and therefore bears no relationship to the present field direction. Ferrous objects consisting of many small, independently fabricated parts do not have a consistent remanence direction. This produces partial cancellation of remanence vectors and a decrease in the importance of permanent magnetization. On the other hand, objects that are fabricated in one piece, or whose mass is dominated by such a piece, may carry substantial permanent magnetization, provided the ferrous material is capable of carrying stable remanence.

Permanent magnetization is also affected by self-demagnetization, but is not constrained by an upper limit, in contrast to induced and viscous magnetizations. Let the intrinsic permanent magnetization of a material be J_o. When an object consisting of this material is placed in zero applied field, the internal field is $-NJ_{PERM}$, where J_{PERM} is the observed permanent magnetization. This internal field acts via the intrinsic susceptibility, k_i, to reduce the magnetization of the object (refer to Figure 12). Thus the observed permanent magnetization of the object is given by:

FIGURE 12
(a) Relationship between the internal and external B and H fields for a magnetized ellipsoid. The Gaussian (CGS) system is used. The magnetization J produces poles on the surface of the ellipsoid, which give rise to a demagnetizing field $H_D = -NJ$ directed opposite to J. The resultant internal field, H, is the vector sum of the external field, H_0, and the demagnetizing field, H_D. Induced plus viscous magnetization is limited by self-demagnetization to a maximum value of $J = H_0/N$. For this value, the internal field, to which the susceptibility and viscous remanence responds, vanishes.
(b) Behaviour of B and H fields in the presence of a magnetizable sphere. Note the magnetic flux lines (field lines of B) preferentially travel through the permeable material, producing a more intense B field within the body. By contrast, the internal H field is reduced by self-demagnetization, as explained in (a).
(c) Behaviour of the magnetic flux density B in the vicinity of a permeable ellipsoid.
(d) Configuration of the magnetic flux density B for a hollow permeable cylinder in a uniform applied field. Note the concentration of flux lines within the high permeability walls, and the shielding of the applied field within the cavity (after Jackson, 1975).

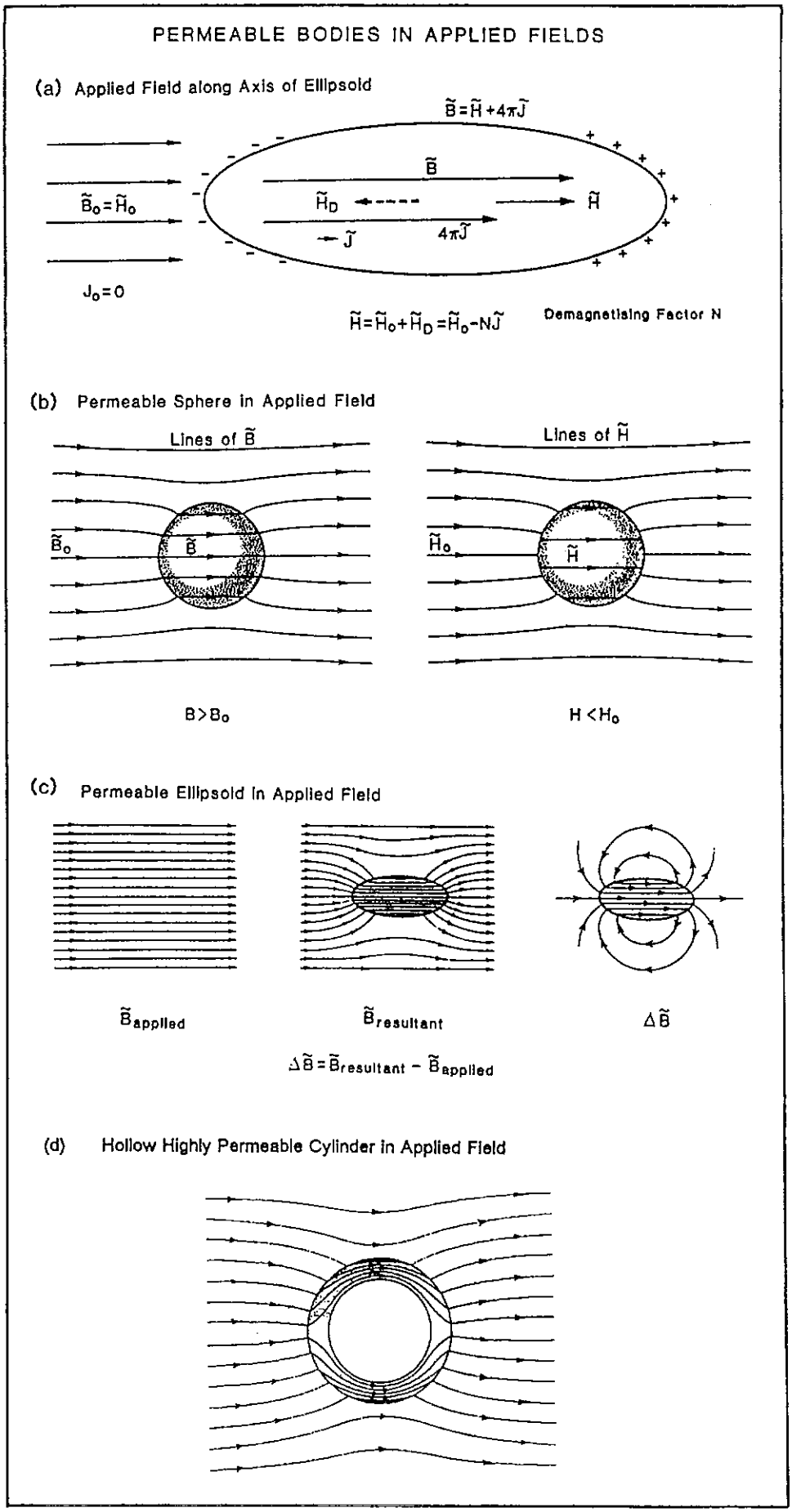
PERMEABLE BODIES IN APPLIED FIELDS
(a) Applied Field along Axis of Ellipsoid
$\tilde{B}=\tilde{H}+4\pi\tilde{J}$
$\tilde{B}_o=\tilde{H}_o$
$\tilde{B}$
$\tilde{H}_D$
$\tilde{H}$
$\tilde{J}$
$4\pi\tilde{J}$
$J_o=0$
$\tilde{H}=\tilde{H}_o+\tilde{H}_D=\tilde{H}_o-N\tilde{J}$
Demagnetising Factor N
(b) Permeable Sphere in Applied Field
Lines of $\tilde{B}$
Lines of $\tilde{H}$
$\tilde{B}_o$
$\tilde{B}$
$\tilde{H}_o$
$\tilde{H}$
$B>B_o$
$H<H_o$
(c) Permeable Ellipsoid in Applied Field
$\tilde{B}_{applied}$
$\tilde{B}_{resultant}$
$\Delta\tilde{B}$
$\Delta\tilde{B}=\tilde{B}_{resultant}-\tilde{B}_{applied}$
(d) Hollow Highly Permeable Cylinder in Applied Field

$$J_{PERM} = J_0 - k_i N J_{PERM},$$

$$\therefore J_{PERM} = J_0/(1 + Nk_i).$$

This shows that the observed remanence and observed susceptibility are reduced by the same self-shielding factor, $1/(1 + Nk_i)$, with respect to their intrinsic values.

Laboratory and Field Tests on Steels

Thin strips of steel were cut by angle grinder and tin snips from four drums of the type used in these surveys, for measurements of the magnetic properties. Susceptibilities were measured using a transformer bridge and remanent magnetizations were measured using a CTF cryogenic magnetometer. Susceptibilities were measured along the long axes of the thin strips, in order to minimize self-demagnetizeation. The measured susceptibilities ranged from 4.5 to 6.6 G/Oe (57-83 SI) for strips from a 50 litre chlorine drum, a 20 litre drum and a 5 litre kerosene tin. Strips from the 200 litre drum (no. 9) had somewhat lower susceptibilities, 1.5-2.8 G/Oe [19-35 SI]. Remanent intensities were very variable, and were found to change appreciably after storage in zero field for two weeks. The Koenigsberger ratios calculated from the measured remanence intensities and susceptibilties ranged from 0.05 to 0.2 for the 50 litre, 20 litre and 5 litre drum samples and from 0.1 to 0.5 for strips taken from the side wall of the 200 litre drum. A strip cut from the welded top of the 200 litre drum, however, had a high Koenigsberger ratio of 2.6. This may reflect the effect of welding and is probably unrepresentative of the properties of the bulk of the drum.

Drum rotation experiments were carried out at site B to estimate induced and remanent magnetizations for a 50 litre drum of the same make as the drum buried at site B and for the 200 l no.9 drum from site A. Because the remanent magnetization rotates with the drum when it is rotated, whereas the induced magnetization remains unchanged, measurements of the anomalous field at a fixed point can determine the effects of induced and remanent magnetization separately. The protocols used for these measurements will be described elsewhere (Clark and Emerson, *Explor. Geophys.*, in prep.). The method assumes that the induced magnetization is parallel to the ambient field, which in practice requires that the source is reasonably isotropic magnetically. This assumption is reasonable, given that the observed anomalies over these drums appear consistent with magnetization parallel to the Earth's field.

For a 50 litre drum of mass 3.8 kg, similar to the one used at site B, the following properties were determined:

$$m_{IND} = 3020 \text{ Gcm}^3 \text{ [= 3.02 Am}^2\text{]}$$

$$\therefore J_{IND} = 3020 \text{ Gcm}^3 \times (8 \text{ g/cm}^3)/3800 \text{ g} = 6.36 \text{ G [= 6.36 kA/m]},$$

$$k = 6.36 \text{ G}/0.58 \text{ Oe} = 11.0 \text{ G/Oe [= 138 SI]}$$

$$m_{NRM} = 675 \text{ Gcm}^3 \text{ [= 0.675 Am}^2\text{]}$$

$$\therefore J_{NRM} = 675 \text{ Gcm}^3 \times (8 \text{ g/cm}^3)/3800 \text{ g} = 1.42 \text{ G},$$

$$D_{NRM} = 5°; I_{NRM} = +29°,$$

$$Q_{NRM} = 1.42 \text{ G}/6.36 \text{ G} = 0.22,$$

where m refers to magnetic moment, J to magnetization, k to the observed susceptibility (not including viscous remanence), NRM is the vector sum of the permanent and viscous remanences and Q_{NRM} is the corresponding Koenigsberger ratio. D_{NRM} is the declination of the NRM, measured positive clockwise from a fiducial mark that was parallel to magnetic north during storage of the drum for several days prior to the rotation experiments. I_{NRM} is the inclination of the NRM, positive downwards. These results indicate that the magnetization of this drum is predominantly induced, that the observed susceptibility greatly exceeds the upper limit for a solid quasispherical body and that the remanence is highly oblique to the field direction experienced by the drum during storage. Thus the remanence is predominantly permanent magnetization, rather than viscous remanence, over a time scale of several days at least.

The 200 litre drum no. 9 (mass 18 kg) from site A was found to have the following properties:

$$m_{IND} = 13{,}700 \text{ Gcm}^3 \text{ [=13.7 Am}^2\text{]}$$

$$\therefore J_{IND} = 13{,}700 \text{ Gcm}^3 \times (8\text{g/cm}^3)/18{,}000\text{g} = 6.1 \text{ G[=6.1 kA/m]},$$

$$k = 6.1 \text{ G}/0.58 \text{ Oe} = 10.5 \text{ G/Oe [= 132 SI]}$$

$$m_{NRM} = 5300 \text{ Gcm}^3 \text{ [= 5.3 am}^2\text{]}$$

$$\therefore J_{NRM} = 5260 \text{ Gcm}^3 \times (8 \text{ g/cm}^3)/18{,}000 \text{ g} = 2.34 \text{ G},$$

$$D_{NRM} = 190°; I_{NRM} = -24°,$$

$$Q_{NRM} = 2.36 \text{ G}/6.1 \text{ G} = 0.38.$$

The observed susceptibilities of the two drums, determined by the drum rotation experiments, are therefore very similar. The magnetization of the 200 litre drum is also dominated by the induced component, but the remanence contribution is relatively larger. Again, the remanence appears to be predominantly stable. It is notable that the bulk susceptibilities determined by the drum rotation experiments are substantially higher than those measured on small strips cut from drums. This may partly reflect calibration difficulties with the transformer bridge measurements, which used highly magnetic samples of non-standard shape, and neglect of self-demagnetization effects. However, it is also likely that cutting and/or grinding of the strips has produced work-hardening, which increases coercivity, and possibly remanence, but reduces susceptibility in ferromagnetic materials. It appears that representative magnetic properties are quite difficult to obtain from small samples taken from steel drums.

The relatively high susceptiblities observed in the drum rotation experiments imply that the effective demagnetizing factors for thin-walled hollow drums are much less than for solid objects of similar shape. This is to be expected since, whatever the orientation of the drum with respect to the field, a substantial portion of the drum wall will have a large

component of the field parallel to the local plane of the wall. A rather simple-minded picture of net effects of self-demagnetization, that ignores interactions between different parts of the drum, is adequate for the present discussion. The field component in the plane of the wall magnetizes the metal relatively easily. Whereas the perpendicular component is attenuated by self-demagnetization. The result is that the magnetization tends to be deflected towards the plane of the wall.

More rigorous analysis of the behaviour of highly magnetic thin shells shows that most of the ambient magnetic flux is channelled through the magnetic walls, producing the well-known shielding effect in the hollow interior of such shells. Because the magnetic flux can find a path of low reluctance through the walls of a highly magnetic hollow sphere, avoiding the interior (refer to Figure 12d), the induced magnetization within the walls themselves reflects a concentration of magnetic flux and is therefore relatively intense compared to the uniform magnetization of a solid sphere. It follows that self-demagnetization is much less effective for the hollow sphere than for a solid sphere. This principle can obviously be generalised to other shapes.

In the present experiments the vertical component of the field is ~52,000 nT, the horizontal component is ~25,000 nT. For an upright drum there is negligible self-demagnetization for the vertical component of magnetization within the side walls, as it is everywhere in the plane of the wall. Similarly, the horizontal component of magnetization experiences negligible self-demagnetization within the top and bottom of the drum and on the eastern and western flanks. Thus a substantial proportion of the drum carries a strong induced magnetization. This magnetization tends to be steeper than the present field within much of the side walls, but is deflected towards the horizontal within the top and bottom walls. Overall, the total induced moment does not depart very greatly from the ambient field direction.

It is clear that hollow drums have a more effective magnetization per kg than solid bodies of similar mass.

Magnetic Modelling

The form of the measured magnetic anomalies associated with the drums appears to be consistent with magnetization parallel to the present field direction. As discussed above, in principle the induced magnetization and viscous remanence are expected to vary somewhat in direction and intensity throughout a hollow drum, but it is plausible that the overall magnetic moment associated with these magnetizations is directed subparallel to the present field. Substantial permanent magnetization on the other hand, should produce anomaly shapes that depart significantly from those observed, unless the drum is fortuitously oriented with the permanent magnetization subparallel to the field. In the case of 200 l drum no. 5 at site B, the remanence exactly cancelled the induced magnetization.

Three source geometries were used to model the observed anomalies for the 200 litre drum at site A:

(i) a sphere with radius arbitrarily taken as 0.5 m, which represents the drum as equivalent to a point dipole located at the centre of the drum;

(ii) a solid cylinder, of the same size and shape as the drum;

(iii) a realistic representation of the actual distribution of magnetic material, consisting of a thin annular cylinder (the side walls) plus thin discs (the top and bottom). The thickness of the drum walls was arbitrarily taken to be 1 mm.

Algorithms for calculating magnetic anomalies for these source geometries are given in Emerson et al. (1985). Magnetization by induction was assumed for all the modelling. Nominal model susceptibilities were chosen to give the total magnetic moment required to match the anomaly amplitude at 2.5 metres sensor height, using the type (iii) model. Self-demagnetization was neglected. The nominal susceptibilities for each of the model types are:

(i) 0.0444 G/Oe [0.558 SI] for the sphere, which has a volume of 0.5236 m^3,

(ii) 0.1 G/Oe [1.26 SI] for the solid cylinder, which has a volume of 0.2325 m^3.

(iii) 10.91 G/Oe [137 SI] for the hollow drum model, which contains 2132 cm^3 of magnetic material (equivalent to a mass of 17.1 kg for a density of 8 g/cm^3).

For each of these models the magnetic moment induced by the Earth's field (F = 0.58 Oe = 58,000 nT) is 13,485 Gcm^3 [13.485 Am^2). The CGS magnetic moment m = kFV, where V is the volume in cm^3.

Figures 13, 14, 15 show calculated anomalies for these models. It is evident that all three models produce very similar anomalies, although the sphere (point dipole) model produces a slightly lower amplitude anomaly than the hollow drum model, while the solid cylinder anomaly has intermediate amplitude. The anomaly shapes are practically indistinguishable (Figure 15). This implies that for 2.5 metres sensor clearance the sphere model provides a good representation of a 200 litre drum. Thus a drum of this size is essentially equivalent to a point dipole source for surveys with ground clearance or 2.5 metres, or greater. The sphere model is convenient and is computationally efficient compared to cylinder models. This suggests that, if modelling is required as an aid to locating buried drums, sphere models may serve the purpose very well. The magnetic moment required to best match the observed anomaly amplitude would not need to be slightly higher for sphere models than for models that use the true source geometry.

It is evident from Fig. 13 that the theoretical anomaly based on the hollow drum model fits the observed profile very well for 2.5 metre sensor height. Figure 14 confirms that there is also a very good match between theoretical and observed anomalies for 3.5 metres sensor height, using the identical model geometry and magnetic moment. Sphere models with slightly higher moments also give acceptable fits. At 2.5 m sensor height the drum top contributes about 20 nT to the

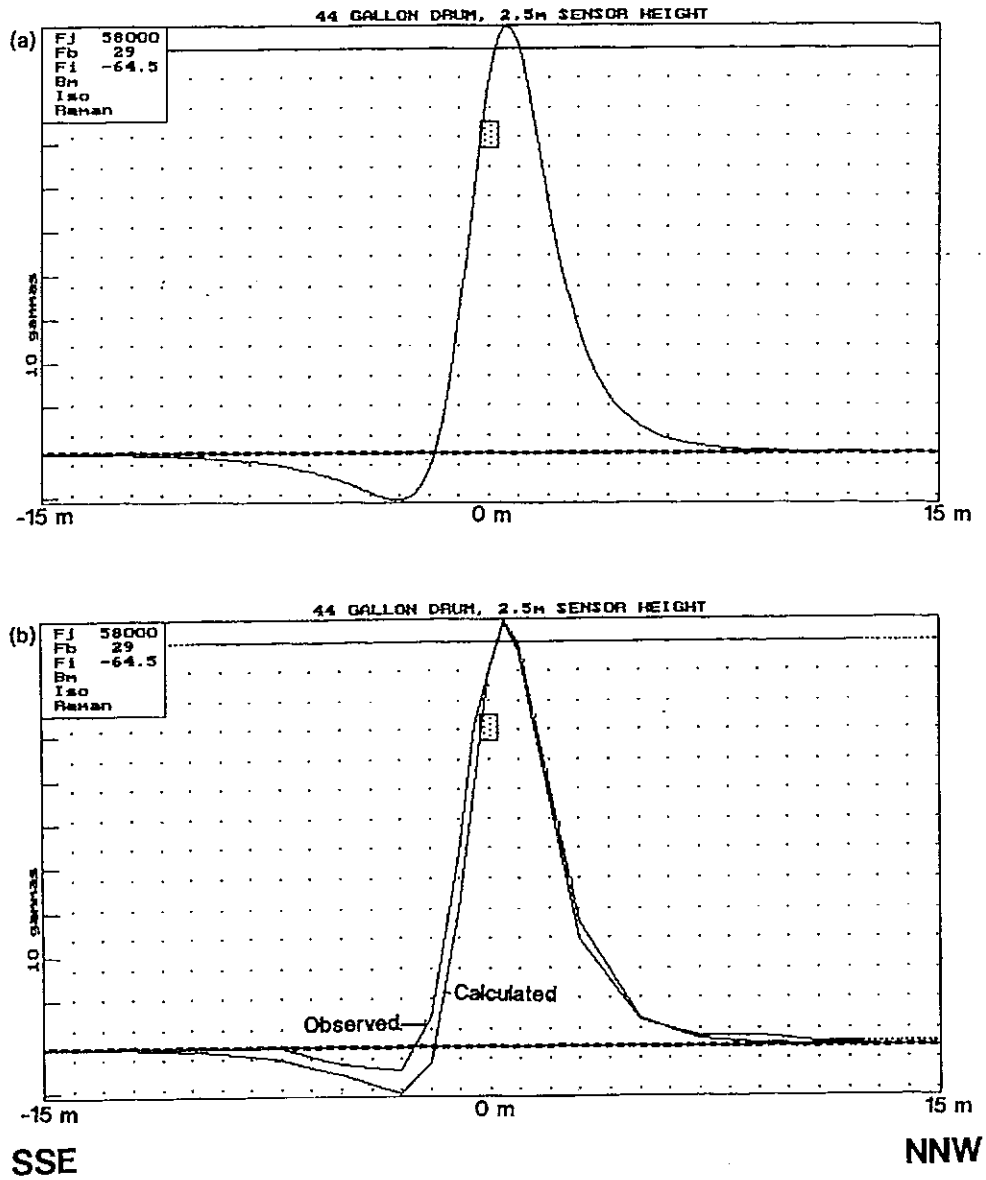

FIGURE 13
Theoretical and observed anomalies for the 200 l drum at site A for 2.5 m sensor height. The top diagram (a) shows the theoretical anomaly over a hollow drum with total magnetic moment chosen to match the observed anomaly amplitude. This anomaly is smooth, having been computed for a large number of stations. The bottom diagram (b) gives a comparison of the observed anomaly at site A with the theoretical anomaly of (a) above. Note that the theoretical anomaly is calculated only at the actual field measurement stations. The y axis gives the anomaly amplitude in gammas (cgs) = nT (SI).

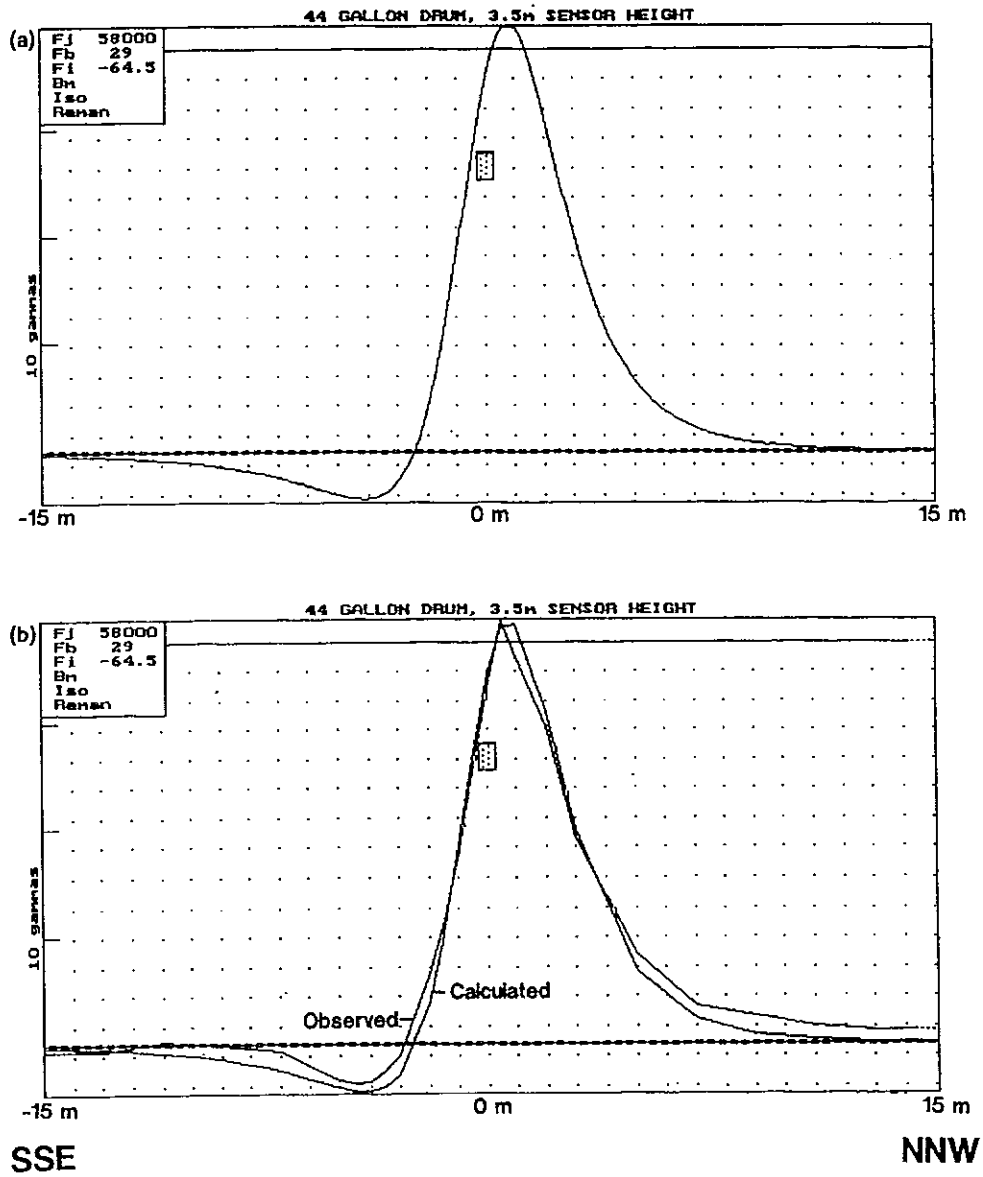

FIGURE 14
Theoretical and observed anomalies for the 200 litre drum at site A for 3.5 m sensor height. The top diagram (a) shows the theoretical anomaly over a hollow drum with total magnetic moment chosen to match the observed anomaly amplitude. This anomaly is smooth, having been computed for a large number of stations. The bottom diagram (b) gives a comparison of the observed anomaly at site A with the theoretical anomaly of (a) above. Note that the theoretical anomaly is calculated only at the actual field measurement stations. The y axis gives the anomaly amplitude in gammas (CGS) = nT (SI).

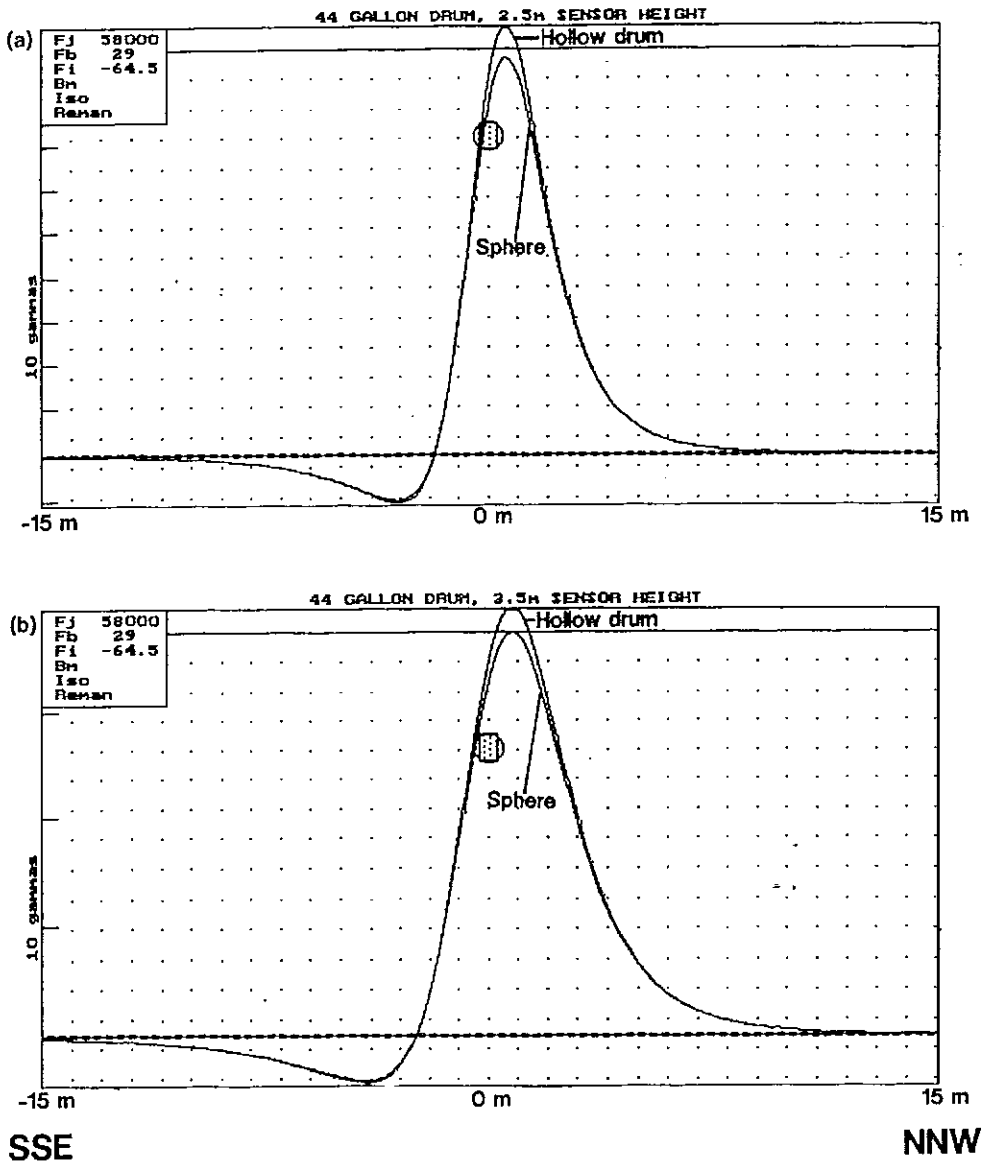

FIGURE 15
Theoretical models of a 200 l steel drum using a sphere and a hollow drum; the anomaly curve for the solid drum lies between these two and has been omitted for clarity. The top (a) plots show a sphere's response together with a hollow drum (the same as for Fig. 13(a)) for a 2.5 m sensor height. The bottom (b) plots are for a 3.5 m sensor height. The y axis gives the anomaly amplitude in gammas (cgs) = nT (SI). Refer to text for further details.

~100 nT theoretical anomaly, whereas the drum bottom contributes about 7 nT. This suggests that an isolated drum lid should be detectable at shallow depths.

Figure 16 and 17 shows calculated and observed anomalies over the 50 litre drum, for sensor heights of 1.5 m, 2.5 m and 3.5 m. Given the smaller size of the 50 litre drum, relative to the sensor distance, compared to the 200 litre drum, a sphere model was used for calculation of the theoretical anomalies. Figure 16 confirms that the 50 litre drum behaves essentially as a point dipole source, with $1/r^3$ fall-off of the anomalous field. This drum is clearly detectable even at the maximum sensor height.

In Figure 16 the model sphere was chosen with a radius of 0.37 m and an assumed susceptibility of 0031 G/Oe [0.39 SI], corresponding to an induced moment of 3815 Gcm^3 [3.815 Am^2], or 1004 Gcm^3 per kilogram of steel. This moment exceeds that calculated from the measured susceptibilities of the thin strips cut from a 50 litre drum by a factor of 3.1. The difference between this measured susceptibility and the in situ effective susceptibility can be nominally attributed to a viscous remanent magnetization (VRM) subparallel to the induced magnetization, with a Koenigsberger ratio (Q) of 2.1. However, the anomalously low measured susceptibility of the drum steel may largely reflect the effect of cutting and calibration difficulties, as discussed in the previous section. The effective susceptibility of the steel, calculated from the dipole moment of the buried drum, is 8 G/Oe [100 SI], compared to 11 G/Oe [138 SI] determined from the drum rotation experiment using a different drum of the same type. The profiles presented in Figure 17 accommodate the effects of a nominal VRM with a Q of 2.1 or, equivalently assume magnetization by induction with a susceptibility 3.1 times higher than the laboratory measured values.

If the magnetic properties determined from the drum rotation experiments are used to calculate the theoretical anomalies, reasonable matches with the observed profiles are obtained for both the 200 litre and 50 litre drums. This confirms that the rotation experiments determined the bulk magnetic properties of the drums with reasonable accuracy. The magnetization of the 50 l drum is predominantly induced and the VRM is minor.

Figure 18 shows calculated and observed anomalies over the 3×3 array of 200 l drums, along a traverse with bearing 050° mag. For simplicity, the drum array was modelled as nine spheres, centred on the actual locations of the drums. The central drum in this array was the same as the drum (no. 9) modelled in Fig. 13 and was therefore given the same magnetic moment in the nine drum model. The remaining eight drums were assigned a common magnetic moment. The magnetic moment assumed for each of these other drums needed to be lower (10,780 Gcm^3 = 1.078 Am^2) than that of the central drum (13,485 Gcm^3 = 1.3485 Am^2), in order to match the observed anomaly. Thus the drum used for the single drum survey at site A is somewhat more magnetic than the average drum in this collection.

For simplicity, a single sphere was used in Figure 19 to model the 3×3 array of drums for a magnetic NE-SW profile. The match between theoretical and observed profiles in this case is not as good as in Figure 18 suggesting that the source geometry in this case is too complex to be well modelled by a single dipole. However, an array of spheres should provide an adequate representation of a cluster of buried drums in most cases.

For isolated drums, the success of the sphere model, even for the largest drum used, arises from a basic principle of potential theory. This states that, at any point lying outside a sphere that completely contains the source, an arbitrary source can be represented by a set of multipoles located at a single point within this sphere. Thus any compact ferrous object is equivalent to a set of multipoles at its centre. This can be expressed:

Source = Dipole + Quadrupole + Octupole + Hexadecapole + . . .

Field Fall-off	$1/r^3$	$1/r^4$	$1/r^5$	$1/r^6$	. . .

Note that for magnetic sources there is no monopole term. For large r the dipole term dominates completely (unless the dipole moment is zero). A uniformly magnetized sphere, or hollow sphere, is a special case, for which the higher order multipoles vanish identically. These sources can be exactly represented by a point dipole at any external point. Bodies of high symmetry, such as uniformly magnetized cubes and cylinders (solid or hollow), have zero quadrupole moment. Therefore thse bodies behave very much like spheres, except very close to their boundaries. Collinson (1983, pp. 210-218) discusses the external fields due to cubic and cylindrical sources. At a distance equal to the cube side from a cube face, the field is within 4% of the field arising from an equivalent centred dipole, and converges rapidly to the dipole field with increasing distance. Similarly, for reasonably equidimensional cylinders, with height/diameter ratios between 0.8 and 0.9, the maximum difference between cylinder and dipole fields is 4% at a distance of a diameter from the cylinder surface, again decreasing rapidly with increasing distance.

Heterogeneous magnetization produces a non-zero quadrupole moment, but the effects fall off rapidly with distance. It is not surprising, therefore, that drums behave essentially as dipole sources at typical sensor distances during environmental surveys. The $1/r^3$ dependence provides a useful rule-of-thumb for estimating expected anomaly amplitudes and maximum depths of detection.

Field Results — TEM and Resistivity, Sites B and E

The GEONICS EM47/PROTEM system employed to carry out shallow transient electromagnetic profiling was laid out as shown in Figures 4 and 20a. Typical decay curves are presented in Figure 20b.

Prior to burying the drums in Sites B and E, test TEM profile was recorded in order to ensure there were no conductors, natural or man-made, already present. The profile for site B,

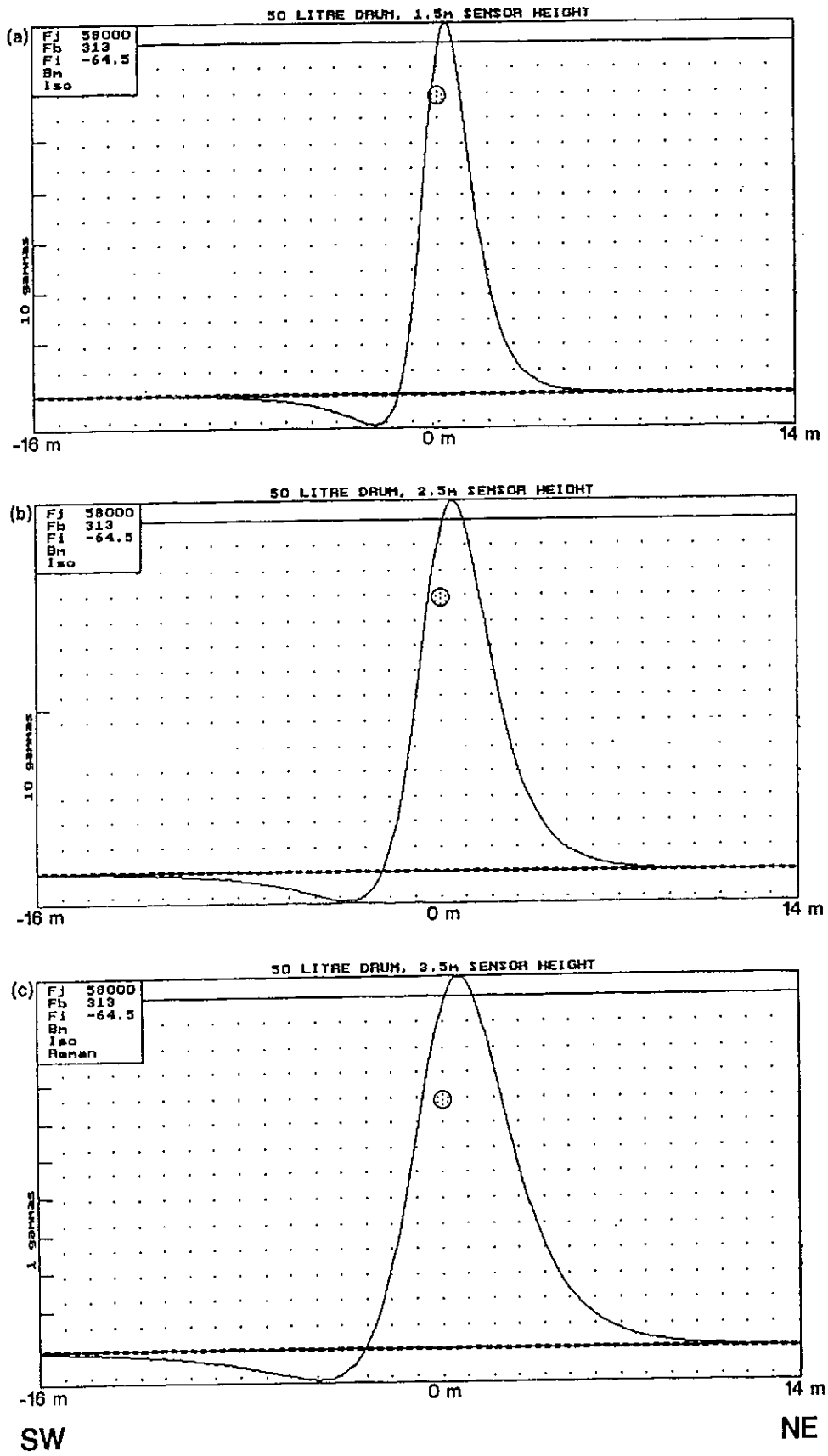

FIGURE 16
Detailed modelling profiles for a sphere of radius 0.37 m and arbitrary susceptibility 0.031 G/Oe [0.39 SI] chosen to provide a match to the total magnetic intensity anomaly amplitude of a 50 l steel test drum from site B. Total magnetic intensity profiles are presented for 1.5 m, 2.5 m, 3.5 m sensor heights in the top (a), middle (b) and bottom (c) panels. These profiles show the dipole character of the response. The y axis gives the anomaly amplitude in gammas (cgs) = nT (SI).

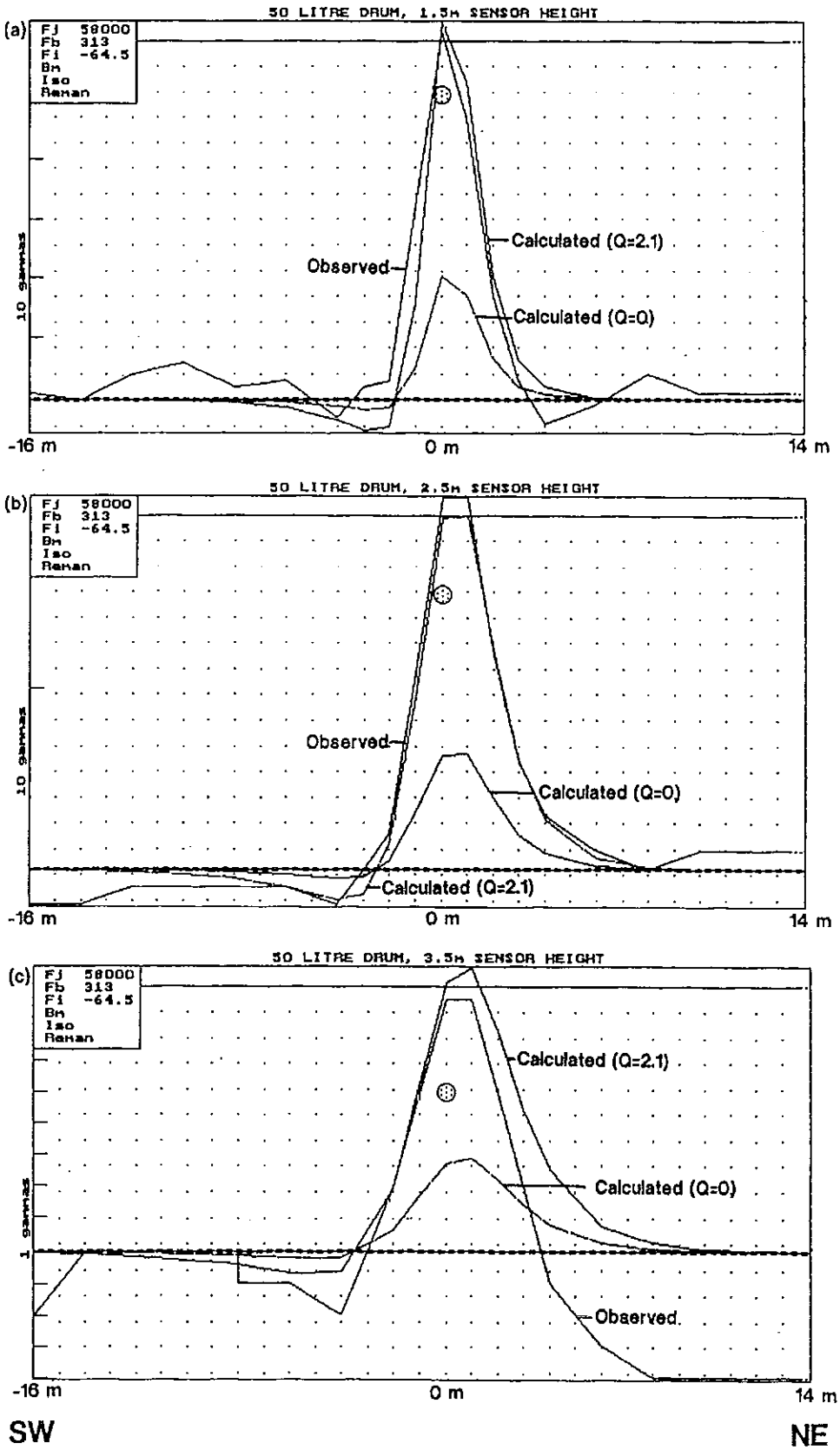

FIGURE 17
Comparison of the theoretical and observed anomalies at field stations for a 50 litre steel drum at site B. The top (a), middle (b) and bottom (c) panels are for sensor heights of 1.5, 2.5 and 3.5 m respectively. The anomaly calculated from the measured susceptibility of thin metal strips corresponds to the curves marked Q = 0. The curves marked Q = 2.1 indicate the theoretical curves that best match the observed anomaly amplitudes; these require effective susceptibilities 3.1 times larger, equivalent to a viscous remanence with a Koenigsberger ratio of 2.1. However, the measured susceptibility of the thin steel strips is not representative of the drum steel. The true susceptibility of the drum steel is considerably higher and accounts for the anomaly.

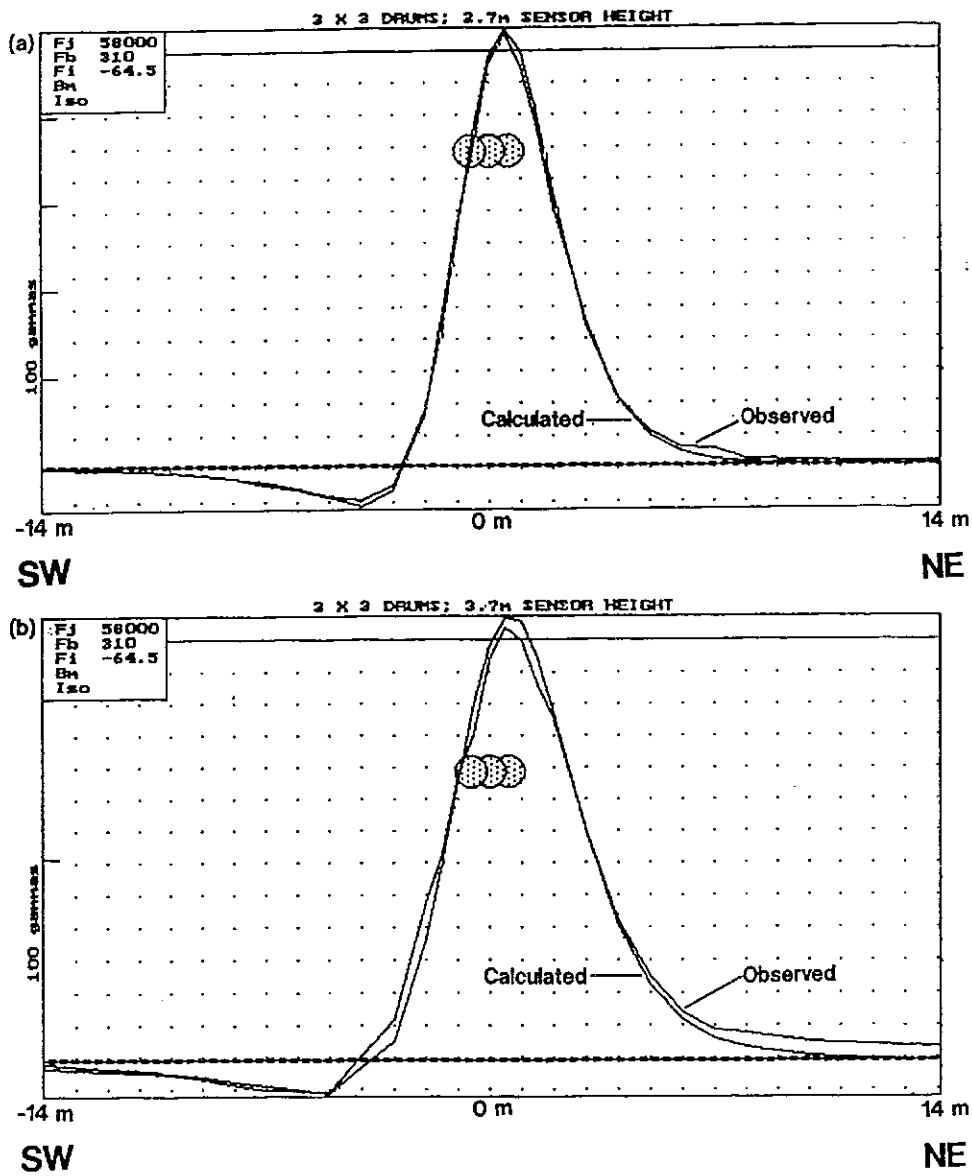

FIGURE 18
A cluster of nine 200 l steel drums modelled as a 3 × 3 array of spheres. Total magnetic intensity anomaly profiles are shown for calculated and observed values for 2.7 m and 3.7 m sensor heights in the top (a) and bottom (b) panels respectively. The y axis gives the anomaly amplitude in gammas (cgs) = nT (SI).

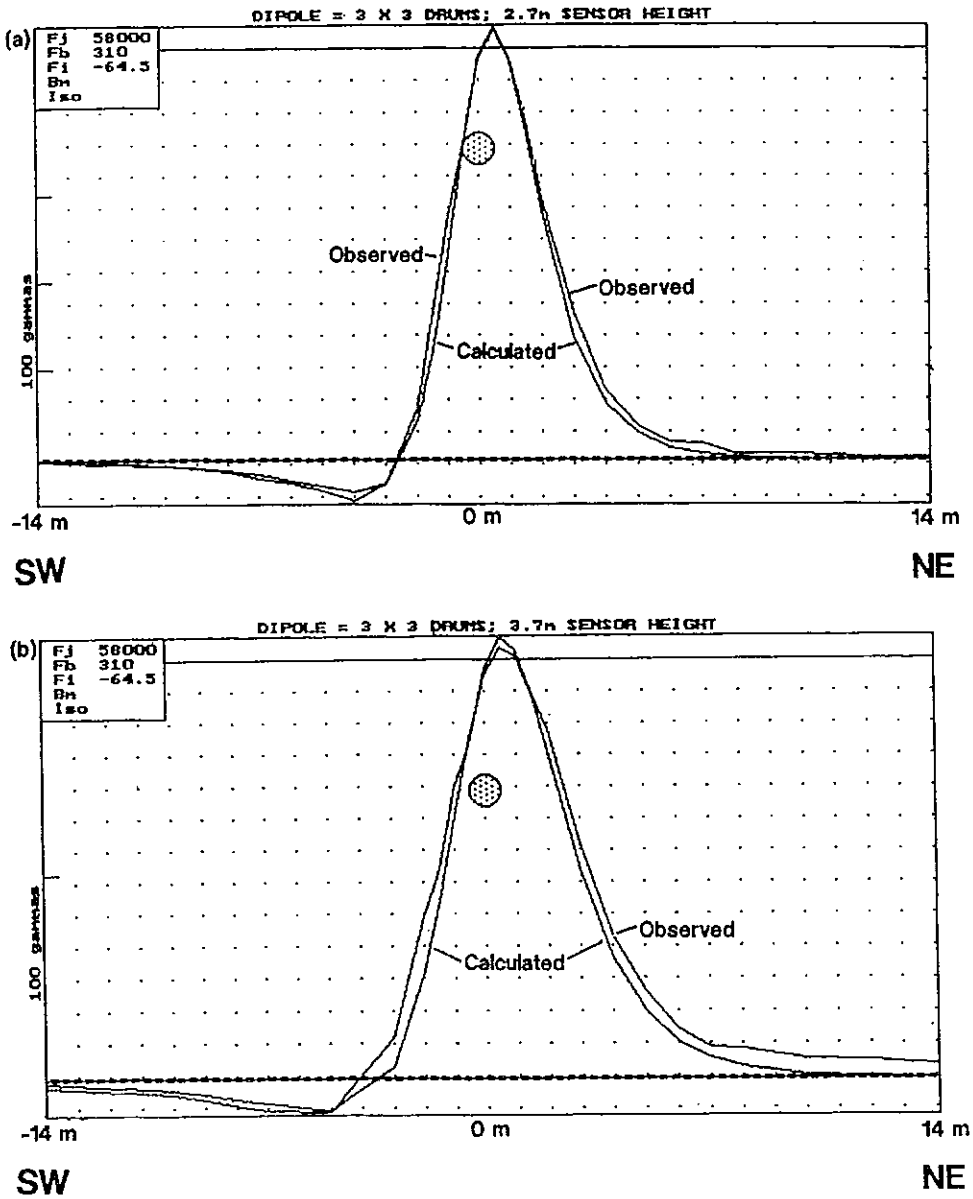

FIGURE 19
A cluster of nine 200 l steel drums modelled as a single dipole or sphere. Total magnetic intensity anomaly profiles are shown for calculated and observed values for 2.7 m and 3.7 m sensor heights in the top (a) and bottom (b) panels respectively. The y axis gives the anomaly amplitude in gammas (cgs) = nT (SI).

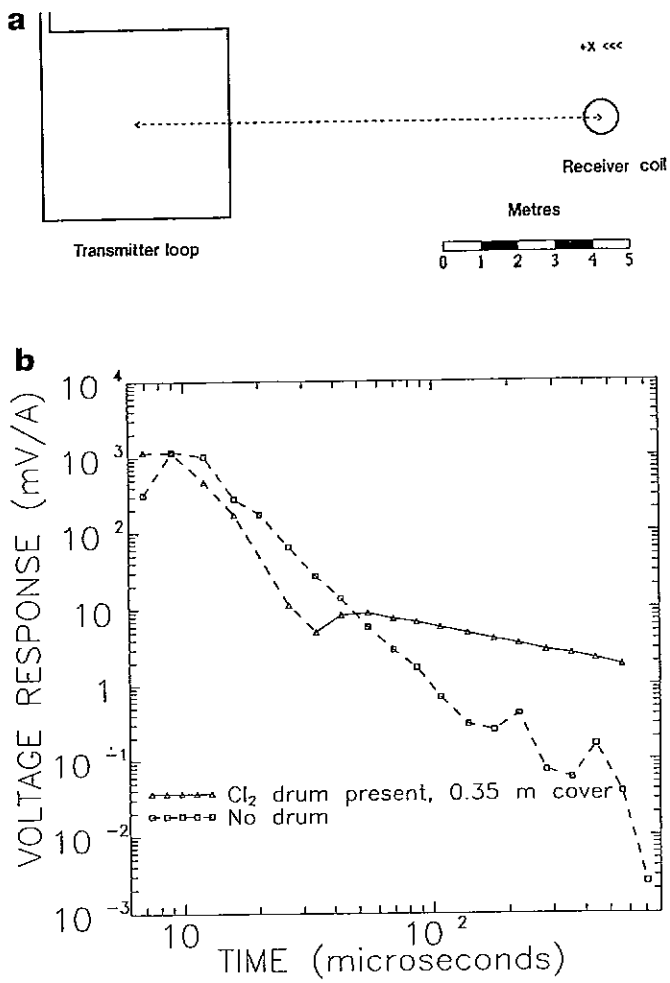

FIGURE 20
The top (a) diagram shows the transmitter-receiver configuration used to acquire the TEM profiles on site B and E. This is the standard "offset sounding" configuration (Geonics, 1991). The transmitter and receiver were moved simultaneously along each survey line, with the distance between the transmitter and receiver centres kept constant at 12.5 m. The bottom (b) diagram presents two typical TEM decays observed in Area B, one recorded over barren ground and one with the receiver positioned immediately above the buried 50 l steel drum. Dashed lines indicate negative voltages. Note the change in sign of the decay associated with the presence of the conductive drum. The PROTEM receiver was operated at the UH frequency (see Appendix) for both measurements.

is shown in Fig 22a. Transformation of these data to late-time apparent resistivity indicated resistivities at late channel times of approximately 125 Ωm at the southwestern end of the profile, and of 200 Ωm between 15 N and 40 N. Near surface apparent resistivities between 15 N and 40N were approximately 100 Ωm. A 50 l steel chlorine drum was subsequently buried at 29.85 N, and laboratory measurements on soil samples taken from the pit gave the resistivities shown in Table 2. These resistivities were a useful guide in assessing the field results. The resistivity of the 50 l drum's steel was estimated to be of the order of 10^{-7}Ωm (Lide, 1991).

Area B, 50 l steel (chlorine) drum

The dimensions of the various drums and their depths of burial are given in Table 3. All of the drums were buried in the upright position for TEM tests. Figure 22b shows an EM-47 profile at a regular station interval of 5 m over a 50 l drum buried at 29.85 N, with additional stations 27.5 N and 32.5 N also recorded. Further tests showed the response from the drum was observable at an offset of 1 m from the drum, but that there was no discernible anomaly at an offset of 2 m. Response directly over the drum was subsequently measured at three different receiver frequencies, and was found to persist until 3.56 msec after transmitter turn off. The amplitude of the response 1 m from the drum at channel times later than 0.101 msec was only a quarter of that directly over the drum. At a distance of 1 m from the drum, the response persisted until a channel time of 1.75 msec.

The TEM response of a cluster of drums would be expected to be greater than that of a single drum, due to the larger effective conductor cross-section (Spies, 1980). The response is, however, a complicated function of transmitter and receiver moments, and of target geometry.

Wenner array galvanic resistivity profiles acquired over the 50 l drum are shown in Fig. 21. Apparent resistivity values are plotted at the centre of the electrode spread i.e. at a point midway between the potential electrodes. Time constraints and the limited availability of the field instrument unfortunately meant that it was not possible to acquire additional data without the drum present. Profiles were recorded using electrode spacings of 1, 2 and 3 m. All three profiles show the same general resistivity trend along the traverse. Resistivities are relatively high at either end of the profile, and there is a broad zone of lower resistivity approximately between 18 m and 34 m. Qualitatively, the data are consistent with the TEM indications and the laboratory results.

Of the three profiles, only that acquired with the electrodes spaced by 1 m shows a distinct anomaly which may be associated with the buried drum, although the anomaly is superimposed on the broader resistivity trend noted above. An apparent resistivity high can be observed immediately over the drum, flanked by two low apparent resistivity values at 29 m and 31 m. Such a "W" shaped anomaly is consistent with that expected for a profile passing over a thin conductive sink/dyke [with thickness/diameter = 0.5 × electrode spacing] in a more resistive earth (Van Nostrand and Cook, 1966). The low apparent resistivity observed at 27 m does not appear to be related to the presence of the drum, and unfortunately confuses the interpretation somewhat. It is quite possible that there is a contribution from the buried drum to the profiles acquired with the larger electrode spacings. The amplitude of the anomaly is however greatly diminished, and it is difficult to distinguish from the background trend.

The interpretation of resistivity profiling data can be quite complicated — a single body can often produce a multi-peaked anomaly (Van Nostrand and Cook, 1966). The response of a number of closely spaced buried drums could therefore be expected to exhibit complex characteristics. Depth of penetration in profiling operations is roughly equal

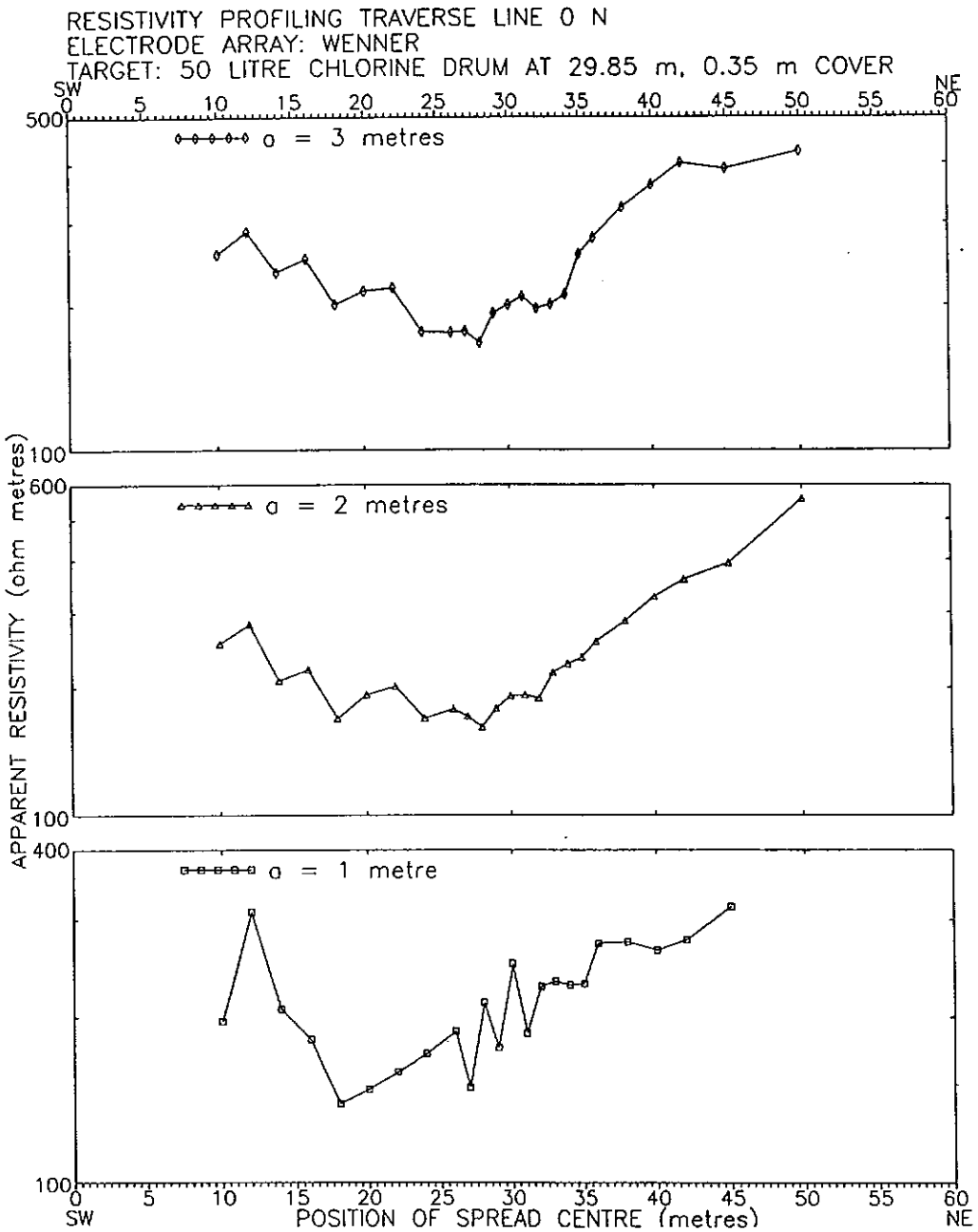

FIGURE 21
Wenner resistivity profiles over the buried 50 l steel drum located at 29.85 m. Electrode separations of 3 (top), 2 (middle) and 1 m (bottom) were used. The presence of the drum is inferred from the jagged response around 29 m on the traverse line with the 1 m spacing. The y axis apparent resistivities are on a log scale.

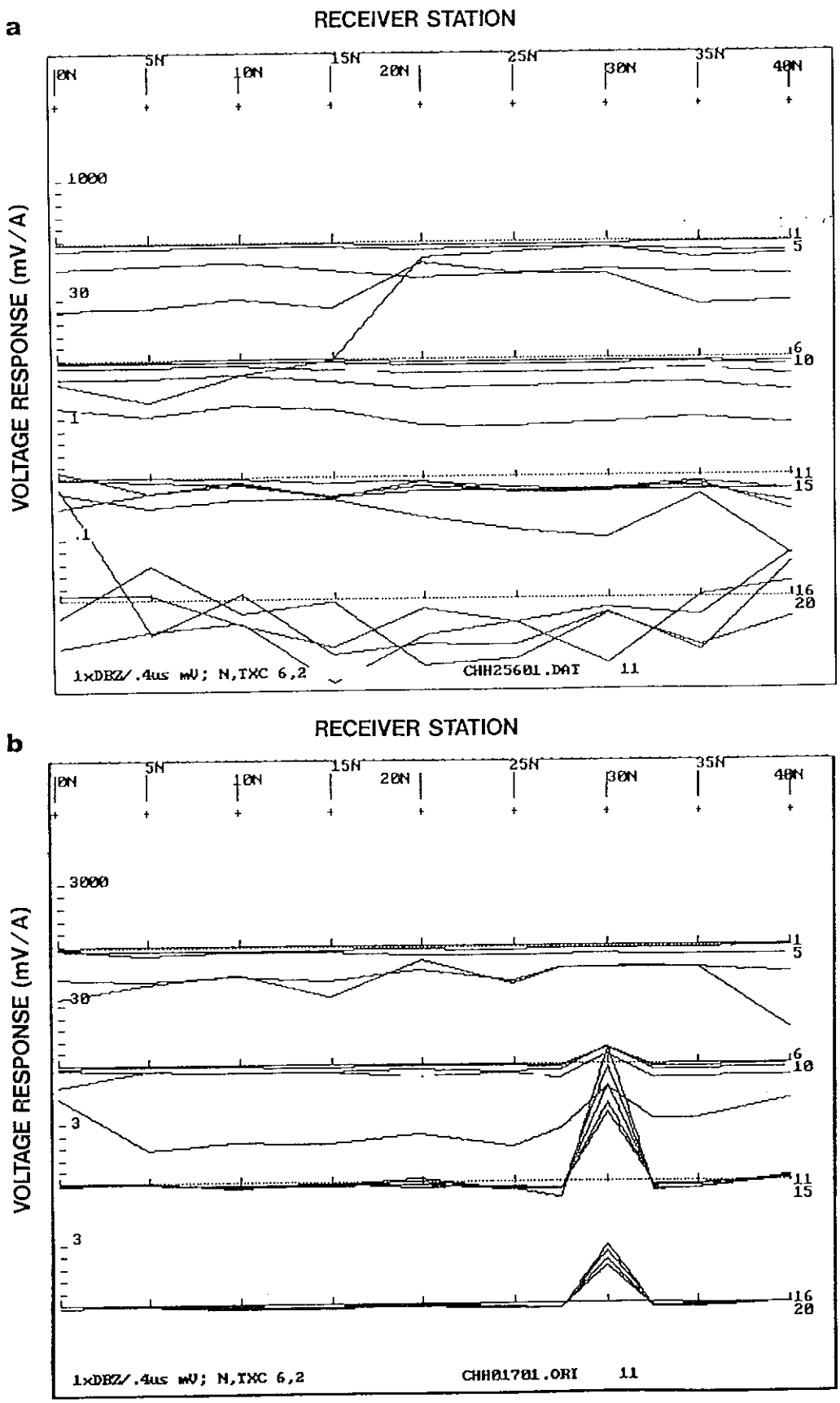

FIGURE 22
The top (a) diagram shows the EM-47 test profile recorded at the first 19 receiver channels only. Channel 20 was used to record the primary magnetic field and has not been plotted. The bottom (b) plots are from the repeat survey of the line with the drum buried at 29.85 N. The response from the drum can be clearly observed at station 30 N and persists until receiver gate 19 (gate centre time 561 μsec). No response from the drum is evident at receiver stations 27.5 N and 32.5 N. The absolute value of the voltage response is plotted on both profiles.

to 0.6 times the Wenner spread electrode spacing (van Nostrand and Cook, 1966).

Area E, plastic and small steel drums

Figure 23a shows a profile at a 1 m station spacing over a 5 l steel drum buried at 4 N in Area E. Although there is a definite response immediately over the drum, there was no discernible response at an offset of 0.5 m. The response immediately over the tin was detectable until a channel time of 354 μsec. There was no significant modification of the response when the survey was repeated with the tin full of saline water of resistivity 0.2 Ωm at 15°C.

Measurements were also carried out over a 20 l steel drum. The response of the drum could be detected at an offset of 0.5 m, but no response could be detected at an offset of 1 m.

Response directly over and 0.5 m from the tin persisted until a channel time of 1.44 msec.

A profile was carried out over a 20 l plastic drum filled with salt water. The saline solution had a resistivity of 0.17Ωm at 15°C, and was intended to simulate chemical waste. Figure 23b shows the profile obtained over the plastic drum buried at 4 N. No response from the drum was detected. A much larger (70 l) plastic drum filled with an identical saline solution was tested in air with the PROTEM receiver positioned 30 cm above. Again, no response from the plastic drum was observed.

Discussion

Although it is possible to detect drums buried at shallow depth with TEM, the method is considerably more labour intensive than magnetic profiling. The measurements carried out on drums buried at shallow depth indicated that the anomaly due to a buried drum is very localised — a receiver station spacing of no more than 1 m would be required in order to detect an isolated chlorine drum with the transmitter — receiver configuration employed in this study. Given a small survey area, a fixed transmitter loop configuration, such as that recommended by Lee and Buselli (1988), would certainly increase survey productivity. The TEM method has the advantage over the proton precession magnetic method that it may be possible to acquire useable data from sources such as aluminium and stainless drums and also from steel drums even in areas with quite considerable powerline noise by increasing the number of transmitter cycles over which data is stacked. The targets in this study were buried at shallow depth, and a strong anomaly was detected immediately over each of the metal drums tested. The effect of increasing target depth is to increase the half width of the anomaly but to decrease its amplitude. Lee and Buselli (1988) noted that a central-loop configuration will give a larger anomaly than a fixed loop configuration, despite its being less practical for field operations.

The extremely early receiver channel times available with the PROTEM system are not essential for this type of survey. An early-time SIROTEM, for instance, should detect the response of all the buried drums tested in this experiment.

The Wenner profiling galvanic resistivity technique appears to be capable of detecting buried metal drums, but further tests are required to provide corroborating or other evidence on the routine suitability of the Wenner and other arrays for this type of study.

Conclusions

A steel drum buried at shallow depth is a valid target for magnetic surveying. In magnetically quiet surroundings the survey data should be interpretable in terms of the drum location and size and the maximum depth of the drum. A cluster of steel drums should be more readily located, even in noisier environments.

TEM techniques using small loops provide clear indications of the presence of steel drums at shallow depths. Galvanic resistivity profiling appears to be able to locate a steel drum with dimensions comparable to the electrode array spacing and buried at a depth less than the array spacing. However, the resistivity anomaly is not as clear as that recorded by the TEM technique.

The magnetic method should be the primary technique of choice for a steel drum search program. The TEM and resistivity methods are costlier and more cumbersome, but they may perform a useful auxiliary role as required.

Plastic drums cannot be detected by the magnetic method. It would appear that the TEM method cannot detect them either empty or filled with salt water. The use of GPR would seem to be appropriate for this type of target.

This study suggests that magnetization by induction can be assumed for most steel drums. Viscous remanence makes only a minor contribution to the effective susceptibility. Permanent magnetization is present, but makes only a minor contribution to the total magnetization. The effective susceptibility was found to be ~10 G/Oe [~130 SI] for several 200 litre and 50 litre drums. The corresponding magnetic moment is ~700 Gcm^3 [0.7 Am^2] per kilogram or ~700,000 Gcm^3 [700 Am^2] per tonne of steel. The relatively high effective susceptibility reflects relatively small effects of self-demagnetization for thin-walled drums compared to solid objects. The magnetic moments of different drums are quite variable, however, and some drums have moments considerably lower than the above values. The induced moment per unit mass may be an order of magnitude lower than the above values for compact solid ferrous objects, due to self-demagnetization. Thus the anomalies due to compact ferrous objects of different types are not simply proportional to the mass of the source, but are strongly dependent on the source geometry through its effect on the demagnetizing factors.

The sphere model may provide an adequate representation of steel drums for interpretation of environmental surveys. However, self-demagnetization should not be incorporated into the sphere model, because the effective demagnetizing factor is much lower for thin-walled drums than for solid spheres. This implies that the anomalous field due to isolated drums is essentially equivalent to that of a point dipole located at

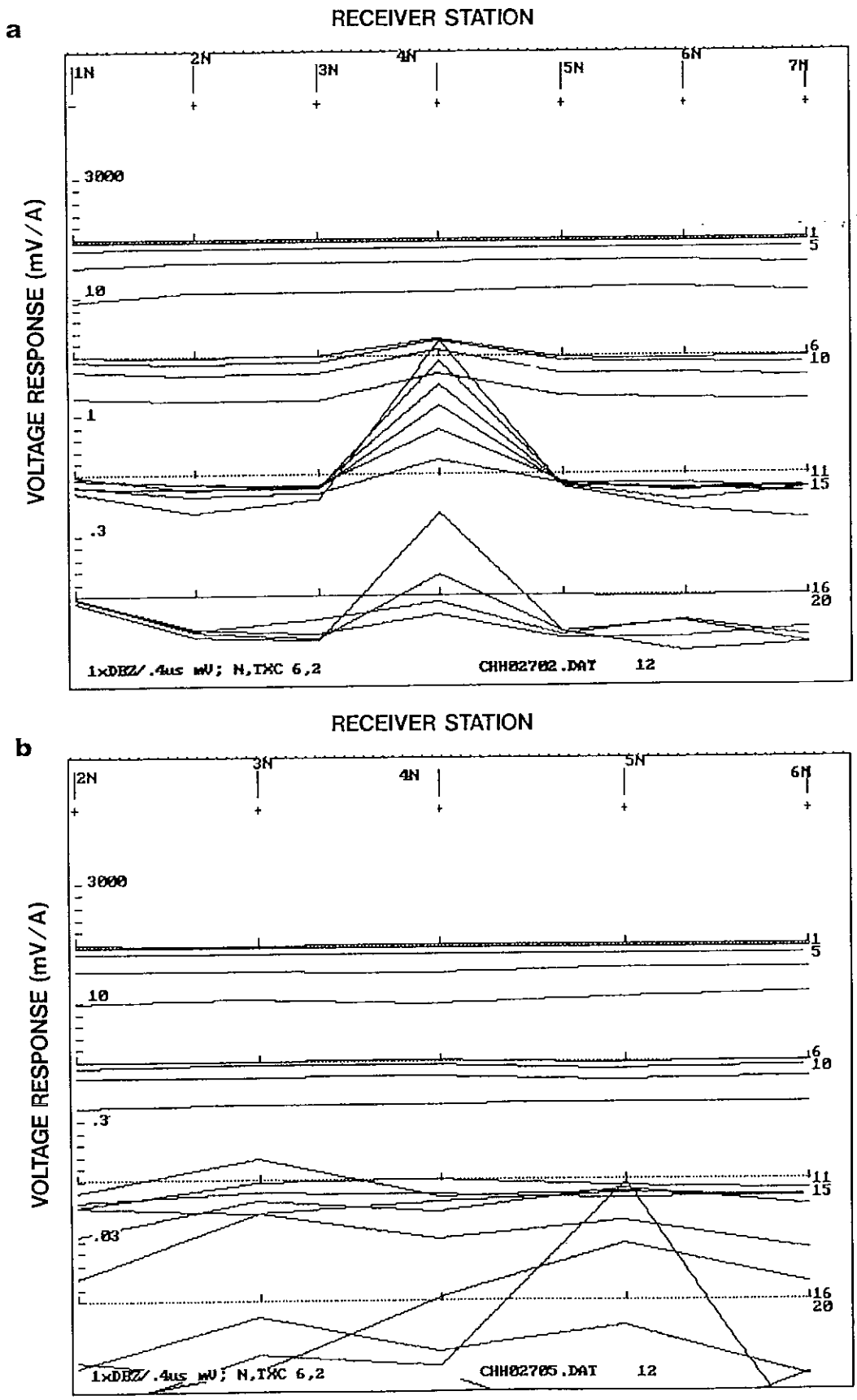

FIGURE 23
The top (a) voltage plots are for the EM-47 profile at 1 m station interval over 5 l steel drum buried at 4 N on site E. The drum response can be easily discerned and persists until receiver channel 19. No response from the drum is evident at receiver stations 3 N or 5 N. The bottom (b) plots show the EM-47 profile over 20 litre plastic drum filled with saline water buried at 4 N on site E. No response from the drum is evident. The apparently prominent spike at late time (channel 18) at station 5N is really low amplitude noise.

the centre of the drum and that the field falls off as the inverse cube of the distance from the centre of the drum. Clusters of drums can be adequately represented by clusters of spheres, but the moments of drums in the cluster may be modified with respect to the moments of isolated drums, due to interactions between adjacent, strongly magnetic sources. In steep geomagnetic fields the anomaly due to a laterally extensive cluster of drums should be lower than the sum of the anomalies due to each drum in isolation. In very shallow fields however, interactions may act to increase the anomaly amplitude.

Based on modelling and the $1/r^3$ rule-of-thumb, large (~200 litre) steel drums similar to those studied here should be detectable in most cases when buried up to ~3.5 metres below the surface, assuming a 10 nT threshold of detectability and a 2.5 metre ground clearance for the sensor. For the detectability threshold of 5 nT, this type of drum should be detectable when top of the drum is as deep as ~5 metres. Smaller drums, similar to the 50 litre drums studied here, should be detectable at depths of up to ~1.5 metres for a 10 nT detectability threshold and a 2.5 metre sensor height. Reducing the sensor height by a metre would obviously increase the depth of detectability by a similar amount, unless geological or cultural noise due to sources at or very near the surface limits the signal to noise ratio of the survey.

Acknowledgements

Grateful thanks are expressed to: Ms D. Bond, for preparing the manuscript; Mr D. Annetts, for helpful discussions on TEM anomalies; Mr Y. Yang, for field assistance; Mr J. Odins N.S.W. Department of Water Resources, for arranging the loan of the Terrameter resistivity unit; the Department of Geology and Geophysics, University of Sydney, for provision of the field equipment and laboratory equipment; and to the Sydney Universities Consortium of Geology and Geophysics Departments for the provision of the TEM unit.

References

Breiner, S. (1973). 'Applications Manual for Portable Magnetometers' GeoMetrics.

Clark, D. A., & Emerson, D. W. (1991). 'Notes on rock magnetization characteristics in applied geophysical studies'. *Explor. Geophys.* **22**, 547-555.

Collinson, D. W. (1983). 'Methods in Rock Magnetism and Palaeomagnetism'. Chapman & Hall.

Emerson, D. W., Clark, D. A., & Saul, S. J. (1985). 'Magnetic exploration models incorporating remanence, demagnetization and anisotropy: HP41C handheld computer algorithms'. *Explor. Geophys.* **16**, 1-122.

Geonics Ltd. (1991). PROTEM 47 operating manual.

Gilkeson, R. H., Gorin, S. R., & Laymon, D. E. (1992). 'Application of magnetic and electromagnetic methods to metal detection'. Proc. Symp. Application of Geophysics to Engineering and Environmental Problems, Vol. 1 SAGEEP'92 309-328.

Jackson, J. D. (1975). 'Classical Electrodynamics'. John Wiley & Sons Inc.

Lee, S. K., and Buselli, G. (1988). 'Transient EM analogue modelling for Korean treasure hunting with the SIROTEM system'. *Geophys. Prosp.* **36**, 976-994.

Lide, D. R. ed. (1991). 'CRC Handbook of Chemistry and Physics'. CRC Press.

Lord, A. E., & Koerner, R. M. (1990). 'Detection of Subsurface Hazardous Waste Containers by Nondestructive Techniques' Noyes Data Corp.

Parker, R. J., (1992). 'Auditing of contaminated land'. *Australian Geomechanics no. 22*, 27-31.

Schlinger, C. M. (1990). 'Magnetometer and gradiometer surveys for detection of underground storage tanks'. *Bull. Assoc. Eng. Geol.* **27**, 37-50.

Spies, B. R. (1980). 'TEM in Australian conditions. Field examples and model studies'. Ph.D. thesis, Macquarie Uni., unpub.

Tyagi, S., Lord, A. E. & Koerner, R. M. (1983). 'Use of a proton precession magnetometer to detect buried drums in sandy soil'. *Jour. Hazardous Materials* **8**, 11-23.

van Nostrand, R. G., & Cook, K. L. (1966). 'Interpretation of resistivity data' United States Geol. Surv. Prof. Paper 499.

Appendix

Geonics PROTEM Receiver Delay Times

The gate centre times for the PROTEM receiver at the 3 different operating frequencies UH, VH and HI are listed in the table below. Profiles in this study were recorded at the UH operating frequency, although selected measurements were made at the VH and HI system frequencies. The listed gate centre times are measured after the end of the turn-off ramp.

GATE	UH (μsec)	VH (msec)	HI (msec)
1	6.9	0.049	0.101
2	9.0	0.057	0.122
3	12.1	0.070	0.152
4	16.0	0.084	0.188
5	20.2	0.100	0.230
6	26.3	0.126	0.291
7	33.8	0.155	0.367
8	42.5	0.190	0.455
9	54.7	0.240	0.575
10	69.3	0.300	0.720
11	86.0	0.365	0.880
12	107.0	0.450	1.080
13	138.0	0.580	1.380
14	175.0	0.730	1.750
15	219.0	0.900	2.190
16	280.0	1.140	2.820
17	354.0	1.440	3.560
18	441.0	1.790	4.370
19	561.0	2.260	5.540
20	707.0	2.850	7.040